nature medicine

Article

https://doi.org/10.1038/s41591-026-04244-6

In vivo generation of anti-BCMA CAR-T cells in relapsed or refractory multiple myeloma: a phase 1 study

Received: 21 July 2025

Accepted: 26 January 2026

Published online: 25 March 2026

Check for updates

Ning An[1,6], Di Wang[1,6], Peiling Zhang[1,6], Jishuai Zhang[2,6], Philippe Parone[3,6], Jianlin Hu[1], Yuhan Bao[1], Li Xu[1], Haitao Ruan[1], Ying Wan[1], Xinyu Wen[1], Yang Gao[1] & Chunrui Li[1,4,5]

In vivo chimeric antigen receptor (CAR)-T cell generation can bypass ex vivo manufacturing and lymphodepletion, potentially simplifying and accelerating access to cellular therapy; preliminary clinical experience supports feasibility and suggests preliminary efficacy. This phase 1, single-arm, open-label trial evaluated the safety and tolerability of ESO-T01, a nanobody-directed, immune-shielded lentiviral vector encoding a humanized anti-B cell maturation antigen (BCMA) CAR, in adults with relapsed or refractory multiple myeloma. ESO-T01 was administered as a single intravenous infusion of 0.2×10^9 transduction units without leukapheresis, ex vivo manufacturing or lymphodepleting chemotherapy. Five heavily pretreated male patients (median three prior lines) were consecutively enrolled and followed for a median of 6.0 months. The trial was stopped early in 2025, and no further enrollment was performed. The primary endpoint was safety and tolerability, and secondary endpoints included efficacy, pharmacokinetics and pharmacodynamics of ESO-T01. No dose-limiting toxicities occurred. All patients developed grade 3 or higher adverse events. Cytokine release syndrome occurred in four patients (three grade 3 and one grade 2) and was managed with corticosteroids, tocilizumab, or supportive care. The most frequent toxicities were transient cytopenias and reversible hepatic enzyme elevations, and three patients experienced grade 2 infections. One patient developed grade 1 immune effector cell-associated neurotoxicity and died from extramedullary lesion-related spinal cord compression. Preliminary antimyeloma activity was observed: four of five patients achieved objective responses, including three stringent complete remissions, with minimal residual disease negativity (10^{-5}) in all evaluable responders (4/4) by day 60. These findings provide preliminary evidence on the feasibility and safety of in vivo CAR-T generation using an immune-shielded vector. ClinicalTrials.gov registration: NCT06791681.

A full list of affiliations appears at the end of the paper. e-mail: cunrui5650@hust.edu.cn

Multiple myeloma is a malignancy of plasma cells that accounts for nearly 10% of hematologic cancers. It is characterized by clonal expansion in the bone marrow and production of monoclonal immunoglobulins, leading to anemia, bone destruction, renal impairment and immune dysfunction[1]. Despite advances with proteasome inhibitors, immunomodulatory agents and monoclonal antibodies, multiple myeloma remains incurable, and most patients ultimately relapse, underscoring a substantial global disease burden[2].

CAR-T cell therapy has reshaped the treatment landscape for hematologic cancers, particularly B-cell-derived malignancies such as multiple myeloma[3]. Among available targets, B cell maturation antigen (BCMA) is notable for its selective expression on malignant plasma cells[4]. Several autologous CAR-T products targeting BCMA—including idecabtagene vicleucel (ide-cel) and ciltacabtagene autoleucel (cilta-cel) (approved in the United States and Europe) as well as equecabtagene autoleucel and zevorcabtagene autoleucel (approved in China)—have demonstrated deep and durable responses in relapsed or refractory multiple myeloma[5–8]. These pivotal studies have established BCMA-directed CAR-T cell therapy as a breakthrough for patients with relapsed or refractory multiple myeloma, yielding high remission rates in advanced disease[3].

However, conventional autologous CAR-T therapies are limited by complex logistics and biological constraints. These approaches require leukapheresis, individualized ex vivo manufacturing and lymphodepleting chemotherapy, resulting in prolonged production times and reduced accessibility, particularly for patients with aggressive disease who cannot wait[9–11]. Allogeneic CAR-T and CAR natural killer platforms have been explored as potential 'off-the-shelf' alternatives, but they remain dependent on ex vivo cell engineering and preconditioning regimens and face challenges such as immunogenicity, limited persistence and safety concerns[12–15].

To overcome these barriers, a new paradigm has emerged: in vivo generation of CAR-T cells through direct infusion of a CAR-encoding vector. This approach enables endogenous T cell reprogramming without leukapheresis, ex vivo manipulation or lymphodepletion[16]. Proof of concept has been demonstrated in preclinical studies using both viral (for example, lentiviral and adenoviral) and non-viral (for example, lipid nanoparticle) platforms, with lentiviral systems offering stable genomic integration and the potential for durable CAR expression[17–21]. Nonetheless, clinical translation remains at an early stage, and key questions regarding immune kinetics, safety and vector–host interactions remain unresolved.

Here we report a phase 1 study of ESO-T01, a replication-incompetent, T cell receptor (TCR) lentiviral vector encoding a humanized, single-domain anti-BCMA CAR. Administered as an intravenous infusion without leukapheresis or lymphodepletion, ESO-T01 represents a distinct in vivo CAR-T platform compared to both autologous and allogeneic approaches. A previous correspondence reported the initial feasibility of the same construct and infusion dose in four patients[22]. The present study is an independent, single-center clinical trial conducted at Tongji Hospital, separate from the previously reported cohort[22]. Although the same construct and infusion dose were used, the enrolled patients differed in their baseline characteristics, and there was no overlap between the cohorts. In addition, this study provides more comprehensive mechanistic data that complement and extend the initial feasibility findings. Building upon this foundation, the present study provides the comprehensive evaluation of the immunologic, phenotypic and safety dynamics of in vivo lentiviral CAR-T programming in humans. We identify a biphasic immune activation profile, characterize longitudinal CAR-T cell phenotypes in the absence of lymphodepletion and report safety events with translational relevance. Collectively, these findings advance in vivo CAR-T cell therapy from conceptual feasibility toward a preliminary framework to inform risk assessment, patient selection and future clinical development.

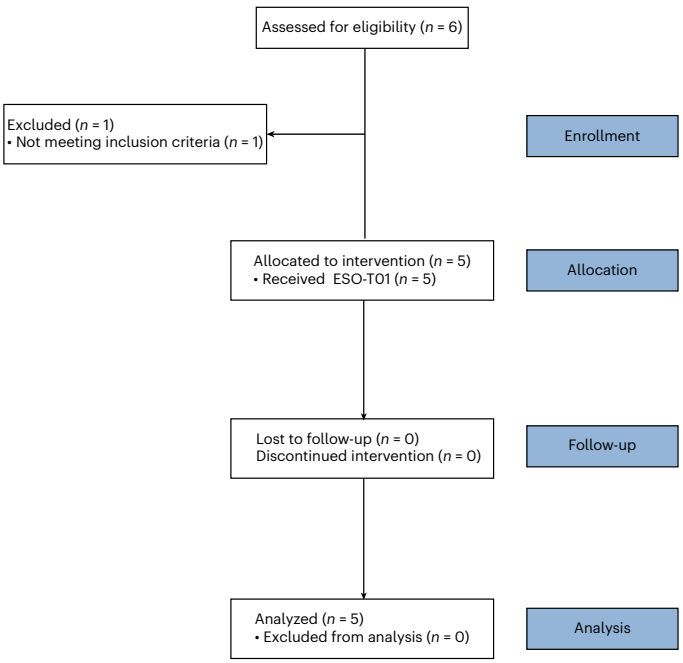

Fig. 1 | CONSORT flow diagram summarizing patient screening, enrollment and treatment in the ESO-T01 study. Six patients were screened between January and March 2025 in Tongji Hospital; one was excluded for not meeting eligibility criteria. Five patients received ESO-T01 infusion and were included in the analysis. No patients were lost to follow-up or discontinued treatment. This CONSORT diagram represents only the Tongji Hospital cohort; the Union Hospital cohort was reported separately in a previous correspondence[22].

Results

Patient disposition and baseline characteristics

Between January and March 2025, six adults with relapsed or refractory multiple myeloma were screened for eligibility. One individual did not meet inclusion criteria and was excluded, resulting in a final cohort of five patients (Fig. 1). The trial was stopped early in 2025 owing to sponsor restructuring, and no further enrollment was performed. The first patient was enrolled on 10 January 2025 and the last patient on 17 March 2025. All five patients received a single intravenous dose of 0.2×10^9 transduction units, without leukapheresis, lymphodepleting chemotherapy, ex vivo cell manipulation or conditioning. Bridging therapy was not permitted. Corticosteroids and antipyretics were allowed at the investigator's discretion but were not mandated.

Baseline demographics and disease characteristics are summarized in Table 1. The median age of patients was 52 years (range, 52–68 years), and all five patients were male (100%). Patients had received a median of three prior lines of therapy (range, 3–5); one patient (I005) could not receive an immunomodulatory imide drug (IMiD) due to a history of lower limb thrombosis; three patients (60%) had previously been exposed to an anti-CD38 monoclonal antibody; and one patient (20%) had undergone autologous stem cell transplantation (ASCT) (Supplementary Table 1). Patient I002 had multiple myeloma with a small pleural effusion at baseline. The interval from diagnosis to enrollment ranged from 4.3 months to 50.1 months. Across the five patients, the median time from enrollment to infusion was 8 hours, 37 minutes (range, 2:00–23:48). The cohort carried a high burden of adverse prognostic features. One participant (I003) had Revised International Staging System (R-ISS) stage III disease and two (I004 and I005) had stage II; R-ISS stage could not be assigned in the remaining two patients (I001 and I002) owing to incomplete cytogenetic information. High-risk cytogenetic abnormalities according to the mSMART criteria—specifically, amp(1q21) and/or del(17p)—were present in patients I003 and I004. Patient I003 also had baseline

https://doi.org/10.1038/s41591-026-04244-6

Table 1 | Baseline characteristics of enrolled patients

Characteristic	I001	I002	I003	I004	I005	Median/summary
Age (years)	52	63	52	52	68	52 (median)
Sex	Male	Male	Male	Male	Male	5/5 (100%) male
Months since diagnosis	4.3	10.5	5.6	43.3	50.1	10.5 (median)
ECOG performance status score[a]	2	2	2	0	0	–
Previous lines of therapy	3	4	3	5	3	3 (median)
Cytogenetic high risk[b]	N/A	N/A	amp(1q21)	amp(1q21), del(17p)	Negative	2/5 (40%)
DS staging	IIIA	IA	IIIA	IIIA	IA	–
R-ISS staging[c]	N/A	N/A	III	II	II	–
Monoclonal protein	IgG-κ	λ free light chain	IgG-λ	IgD-λ	IgA-κ	–
Extramedullary disease[d]	No	No	Yes	No	No	1/5 (20%)
Bone marrow plasma cells at enrollment (%)	25	0.4	60	100	30	30 (median)
Time from enrollment to infusion, h:min	2:00	19:35	2:26	23:48	8:37	8:37 (median)
Prior therapies						
Proteasome inhibitor	Yes	Yes	Yes	Yes	Yes	5/5 (100%)
Immunomodulatory drug	Yes	Yes	Yes	Yes	No	4/5 (80%)
Anti-CD38 monoclonal antibody	No	Yes	Yes	No	Yes	3/5 (60%)
Prior CAR-T therapy	No	No	No	No	No	0/5
Prior auto-HSCT	No	No	No	Yes	No	1/5 (20%)

[a]ECOG performance status scores range from 0 to 5, with higher scores indicating greater disability. [b]Cytogenetic risk was assessed by fluorescence in situ hybridization. High risk was defined as the presence of del(17p), t(4;14), t(14;20), amp(1q21), del(1p) and/or t(14;16). Fluorescence in situ hybridization could not be performed in two patients due to insufficient bone marrow samples. [c]R-ISS stage was derived from ISS stage, presence of cytogenetic abnormalities and serum LDH levels. [d]Extramedullary disease was defined as a soft tissue mass outside the bone marrow. DS, Durie–Salmon staging; auto-HSCT, autologous hematopoietic stem cell transplantation; N/A, not available.

extramedullary disease involving the cervical and thoracic spine. Baseline bone marrow plasma cell infiltration was 60% in patient I003 and 100% in patient I004, underscoring the substantial tumor burden in this early-phase population. Collectively, these characteristics illustrate the advanced, biologically heterogeneous disease treated in this trial.

Primary outcome: safety

Overall safety profile. ESO-T01 was generally well tolerated across the five treated patients (Table 2, Extended Data Figs. 1 and 2, Supplementary Tables 2–5 and Supplementary Fig. 1). Cytokine release syndrome (CRS) occurred in four of five patients (80%, 95% confidence interval: 17–93), including three grade 3 events that resolved within 2 days. One patient (20%) experienced grade 1 immune effector cell-associated neurotoxicity syndrome (ICANS). No dose-limiting toxicities (DLTs) were observed.

The most common adverse events, irrespective of attribution, were transient cytopenias, including lymphopenia (100%), thrombocytopenia (100%), leukopenia (80%) and neutropenia (80%), as well as biochemical abnormalities such as aspartate aminotransferase (AST) increased (100%), gamma-glutamyl transferase (GGT) increased (100%), hypoalbuminemia (100%) and lactate dehydrogenase (LDH) increased (80%). Four patients experienced sinus tachycardia, but no other electrocardiogram abnormalities were observed. Two patients (40%) experienced mild, self-limiting creatinine increased without long-term renal dysfunction. Infectious events included grade 2 herpes simplex virus in two patients within 30 days and one pulmonary infection at 6 months after infusion. Patient I003 required transfusion support for both red blood cells and platelets during cytopenia recovery. All adverse events, including laboratory tests, vital signs, physical examinations and electrocardiograms, are summarized in Supplementary Tables 2 and 3.

Representative clinical course: patient I001. Patient I001, who had a 25% bone marrow tumor burden, received standard premedication with diphenhydramine and acetaminophen prior to ESO-T01

Table 2 | Key adverse events observed during follow-up in five patients treated with ESO-T01

Adverse event	Any grade *n* (%)	Grades 1 and 2 *n* (%)	Grade ≥ 3 *n* (%)
CAR-T-related events			
CRS	4 (80)	1 (20)	3 (60)
ICANS	1 (20)	1 (20)	0
Hematologic toxicities			
Lymphopenia	5 (100)	0	5 (100)
Neutropenia	4 (80)	0	4 (80)
Thrombocytopenia	5 (100)	2 (40)	3 (60)
Leukopenia	4 (80)	1 (20)	3 (60)
Anemia	1 (20)	0	1 (20)
Non-hematologic toxicities			
Fever	4 (80)	3 (60)	1 (20)
Hypotension	3 (60)	3 (60)	0
Hypoxia	3 (60)	0	3 (60)
Sinus tachycardia	4 (80)	4 (80)	0
Hypoalbuminemia	5 (100)	4 (80)	1 (20)
AST increased	5 (100)	1 (20)	4 (80)
GGT increased	5 (100)	5 (100)	0
LDH increased	4 (80)	4 (80)	0
Hyponatremia	3 (60)	2 (40)	1 (20)
Hypocalcemia	4 (80)	4 (80)	0
Hypokalemia	4 (80)	4 (80)	0

Values are shown as number of patients (%). A comprehensive listing of all adverse events by system organ class and grade is provided in Supplementary Tables 2 and 3 and Extended Data Fig. 1.

https://doi.org/10.1038/s41591-026-04244-6

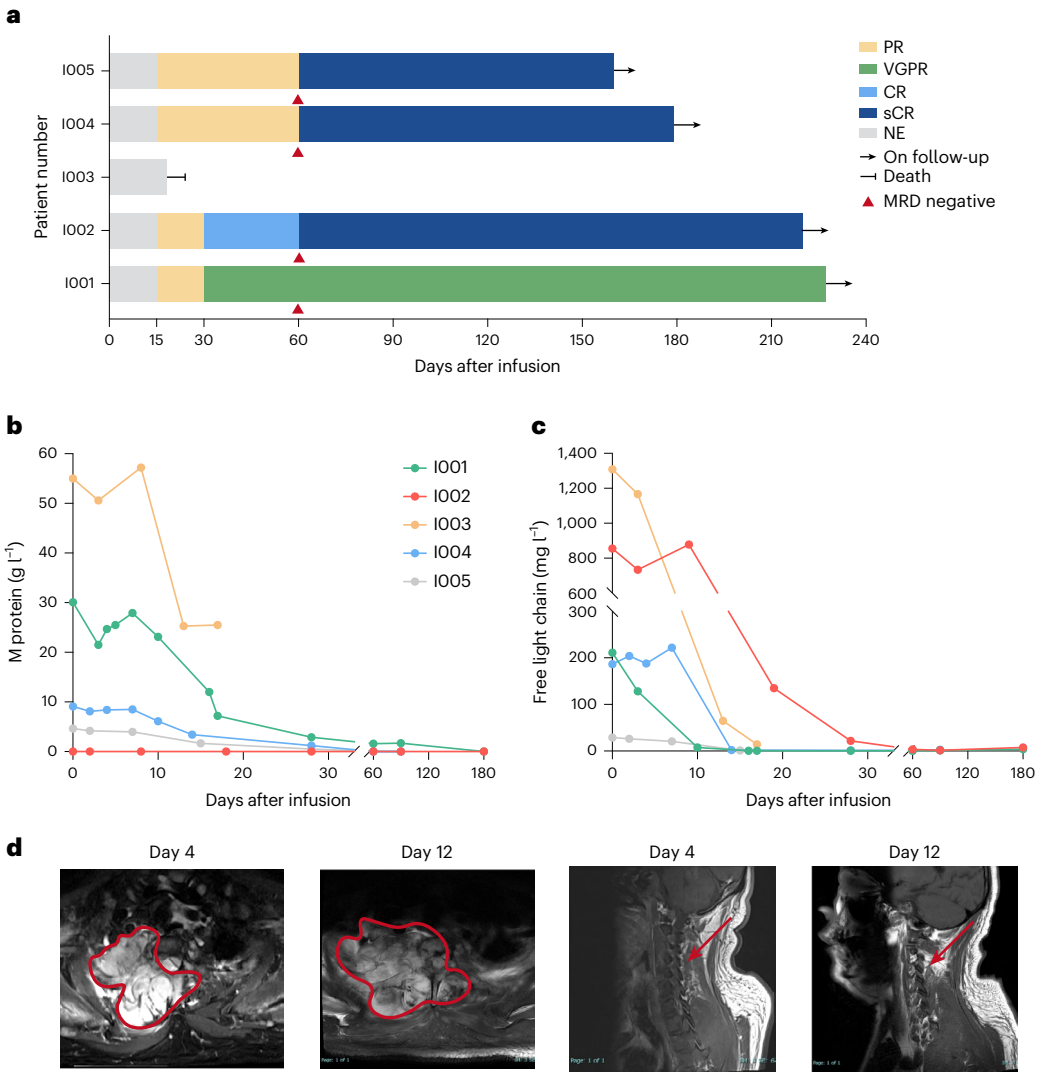

Fig. 2 | Clinical efficacy and biomarker dynamics after ESO-T01 infusion. **a**, Swimmer plot of individual responses according to IMWG criteria. Bars indicate depth and duration of response: PR, VGPR, CR and sCR. Gray segments denote non-evaluable periods. Red triangles mark the first detection of MRD negativity by flow cytometry. Black arrows indicate ongoing follow-up; the vertical bar denotes death (patient I003). **b**,**c**, Longitudinal changes in M protein (**b**) and free light chain (**c**) over 180 days. Patients were monitored according to baseline monoclonal protein type: I001 (IgG-κ), I003 (IgG-λ), I004 (IgD-λ) and I005 (IgA-κ) were assessed by intact immunoglobulin, whereas I002 (λ free light chain) was primarily monitored by serum free light chains. **d**, Imaging changes in patient I003 with extramedullary disease. Left, spine MRI and CT at days 4 and 12 after infusion, with lesion margins outlined in red, showing progression. Right, corresponding MRI and CT demonstrating progressive spinal edema (arrows). CR, complete response; CT, computed tomography; MRI, magnetic resonance imaging; NE, not estimatable; PR, partial response.

infusion. Approximately 2 hours after infusion, he developed an acute reaction characterized by high-grade fever with chills (peak 40.0 °C), sinus tachycardia (130–150 bpm), hypotension (85/49 mmHg) and decreased oxygen saturation (Extended Data Fig. 3a). The patient was managed in the hematology ward, which is equipped for intensive monitoring and emergency interventions and, therefore, was not transferred to the intensive care unit. Immediate supportive measures included high-flow oxygen (15 l min^{-1}), fluid resuscitation and vasopressor support. At emergency evaluation 2 hours after infusion, laboratory testing showed interleukin-6 (IL-6) 3,165 pg ml^{-1}, ferritin 13,363 μg l^{-1}, high-sensitivity C-reactive protein (hs-CRP) 17.7 mg l^{-1} and procalcitonin 0.12 ng ml^{-1}. By 4 hours, these inflammatory markers further increased, peaking at IL-6 > 5,000 pg ml^{-1}, interleukin-8 (IL-8) > 7,500 pg ml^{-1} and ferritin 15,576 μg l^{-1} (Extended Data Fig. 3b). A transient decline in the patient's IgG-κ monoclonal protein was observed, which was interpreted as immune-related fluctuation rather than tumor lysis (Extended Data Fig. 3c).

The patient developed grade 3 CRS 2 hours after infusion. Management included high-dose corticosteroids (dexamethasone 20 mg, three times), tocilizumab (720 mg followed by 400 mg), plasma infusion (400 ml) and two sessions of continuous renal replacement therapy with HA380 hemoperfusion at 6 hours and 24 hours. Dopamine infusion was initiated 12 hours after infusion (3 ml h^{-1}), escalated to 10 ml h^{-1} and discontinued after 30 hours. After these interventions, the patient stabilized, hypotension resolved and inflammatory markers declined. This sentinel inflammatory event prompted a protocol amendment to introduce prophylactic dexamethasone (20 mg intravenously, 1 hour before infusion).

Representative clinical course: patient I003. Patient I003 exhibited baseline lower limb weakness but was able to ambulate with assistance. Motor and sensory functions in the lower extremities were otherwise intact. On the day of infusion, the patient developed grade 1 CRS. By day 3 after infusion, he experienced low back pain, urinary retention,

hypoesthesia and motor dysfunction in the lower limbs, with muscle strength graded as 1. On day 4, complete sensory loss was documented in both lower extremities, accompanied by diminished sensation from the xiphoid process to the lumbar region. By day 6, the sensory deficit had extended below the inter-nipple line, and the patient's CRS had progressed to grade 3 (Extended Data Fig. 4a).

On day 10, peripheral blood analysis demonstrated a peak CAR-T cell copy number of 77,000 copies per microgram of genomic DNA (gDNA). On day 11, coinciding with this peak of in vivo CAR-T expansion, the patient developed acute neurological deterioration, including a transient episode of coma, pinpoint pupils and involuntary movements such as head shaking and tongue protrusion. After intravenous dexamethasone administration, the patient regained full consciousness (Extended Data Fig. 4b–d). Imaging of the spine revealed cervicothoracic spinal cord compression caused by an enlarging epidural mass, and biochemical markers demonstrated marked declines in serum intact M protein (approximately 50%, from 55 g l^{-1} to 25.5 g l^{-1}) and λ free light chains (approximately 90%, from 1,308.8 mg l^{-1} to 14.48 mg l^{-1}). These changes may represent short-lived antitumor activity or immune-related fluctuations (pseudoprogression), although true progression could not be definitively excluded without histopathologic confirmation (Fig. 2d and Extended Data Fig. 4e).

On day 15, the patient developed grade 1 ICANS, manifesting as mild neurocognitive impairment, persistent sensory loss below the xiphoid process and facial and bilateral lower limb edema, although with preserved sensation of urination and defecation. By day 18, he further deteriorated with hypotension and coma, culminating in cardiac arrest on day 19 despite corticosteroid-based supportive care. This sentinel fatal extramedullary lesion compression, which was not observed in the previously reported cohort[22], underscores the importance of anatomical risk stratification before administering in vivo CAR-T cell therapy to patients with preexisting extramedullary disease.

Secondary outcomes

Clinical responses. At the data cutoff (25 August 2025), the median follow-up was 6.0 months (range, 0.6–7.5), and overall outcomes are depicted in Fig. 2a. The overall response rate (ORR) was 80% (4/5), with a median time to response (TTR) of 15 days. Median progression-free survival (PFS), overall survival and duration of response (DOR) were not reached (Supplementary Fig. 2). Patients were monitored according to their baseline monoclonal protein type, and rapid declines in the relevant biomarkers (M protein or free light chains) were observed within the first month after infusion (Fig. 2b,c). Patient I001 achieved a very good partial response (VGPR) by day 30 and maintained this response at the last follow-up. Patient I002 attained a complete response by day 30, which deepened to a stringent complete response (sCR) by day 60. Patients I004 and I005 initially attained partial responses by day 30 and subsequently converted to sCR by day 60. Minimal residual disease (MRD) was assessed by next-generation flow cytometry (EuroFlow panel) with a sensitivity of 10^{-5} and was undetectable on day 60 in all four responders (Extended Data Table 1). Patient I003 experienced a marked decrease in M protein by day 14 after infusion, but extramedullary disease could not be assessed, and the patient died on day 19 due to extramedullary disease-related compression. As of last follow-up, three patients remained in sCR and one in VGPR.

Cytokine dynamics. Cytokine profiling revealed a biphasic inflammatory pattern (Fig. 3). An initial hyperacute cytokine surge occurred within 24 hours of infusion—preceding detectable CAR-T expansion and temporally associated with early CRS onset—followed by a second, more modest peak between days 6 and 14 that coincided with CAR-T expansion and low-grade fevers. This pattern involved early innate cytokines (IL-6, IL-8, tumor necrosis factor (TNF), interleukin-1 beta (IL-1β), ferritin and interferon gamma (IFNγ)) followed by adaptive cytokines (soluble interleukin-2 receptor (sIL-2R), IFNγ, IL-10 and IL-6), indicating sequential innate and adaptive immune activation.

CAR-T expansion and persistence and immune reconstitution. ESO-T01 expansion and persistence were assessed in all infused patients using flow cytometry and quantitative polymerase chain reaction (qPCR). CAR-T cells became detectable in peripheral blood by day 6 in all patients, followed by a marked expansion phase that peaked between days 10 and 14. Peak CAR-T levels ranged from 10.6% to 59.1% of $CD3^+$ T cells, with qPCR values ranging from 77,000 to 220,000 copies per microgram of gDNA and flow cytometry counts from 168.6 to 2,343 cells per microliter (Fig. 4a–b and Extended Data Fig. 5). Corresponding area under the curve from day 0 to day 28 ($AUC_{0–28\,d}$) values indicated durable persistence (315,456–1,301,584 copies · days per microgram of gDNA and 1,137–14,186 cells · days per microliter by flow cytometry). In patient I002, CAR-T cells were also identified in pleural effusion on days 8 and 9, representing 3.2% and 7.8% of $CD3^+$ T cells (Supplementary Fig. 3), suggesting extravascular trafficking. B cell aplasia occurred in all patients by day 10, with recovery by days 60–180 (Fig. 4c). Specifically, B cell recovery was observed in patients I001 and I004 between 2 months and 3 months after infusion, whereas no recovery was detected in patients I002, I003 or I005 during the follow-up period. Natural killer cell and T cell counts exhibited a transient decline restricted to day 1 after infusion (Extended Data Fig. 6a,b). After ESO-T01 administration, serum immunoglobulin levels (IgA, IgG and IgM) decreased within 1 month after ESO-T01 infusion (Extended Data Fig. 6c–e).

Exploratory outcomes

Vector clearance and biodistribution. Quantitative PCR assays detected lentiviral vector DNA in peripheral blood as early as day 2, with complete clearance by day 4. No vector sequences were detected in urine, saliva or feces at any timepoint (Fig. 4d and Supplementary Table 6). Flow cytometry analysis at the time of peak CAR-T expansion showed very low frequencies of CAR^+ cells within $CD3^-$ lymphocyte subsets, monocyte subsets and neutrophil subsets (<1%), providing no evidence of clinically meaningful off-target transduction (Extended Data Fig. 7). Based on ethical and patient safety considerations, organ biopsies were not performed to assess CAR expression. Furthermore, to evaluate genotoxicity risk, integration site analysis was performed on day 12 post-infusion peripheral blood from patient I004, and analysis of a predefined gene set did not show enrichment of integrations near tumor-associated genes relative to background, consistent with a favorable biosafety profile, although longer-term follow-up remains essential (Supplementary Fig. 4).

CAR-T phenotypic and functional profiling. Flow cytometry revealed dynamic changes in CAR-T cell subsets and activation states after infusion. Both $CD4^+$ and $CD8^+$ CAR-T cells expanded in parallel, peaking around day 14, with a balanced $CD4^+/CD8^+$ ratio (Fig. 4e,f). In patient I003, the $CD4^+$ CAR-T count was relatively low, which may have contributed to the limited expansion observed in this case. Early activation markers (CD69 and CD25) peaked between days 4 and 8 and rapidly declined, whereas HLA-DR expression reached its maximum around days 14–17, coinciding with peak CAR-T expansion (Extended Data Fig. 8a,b). Programmed cell death 1 (PD-1) expression rose transiently shortly after infusion but subsequently decreased and remained low by day 30 (Extended Data Fig. 8c). Phenotypic analysis showed a transition from naive and effector states during the first week to central memory (T_{CM}) and effector memory (T_{EM}) subsets by day 28 (Extended Data Fig. 8d,e). Within the $CD8^+$ compartment, T_{EM} cells predominated at later stages, whereas a small pool of naive-like cells reemerged by day 28.

https://doi.org/10.1038/s41591-026-04244-6

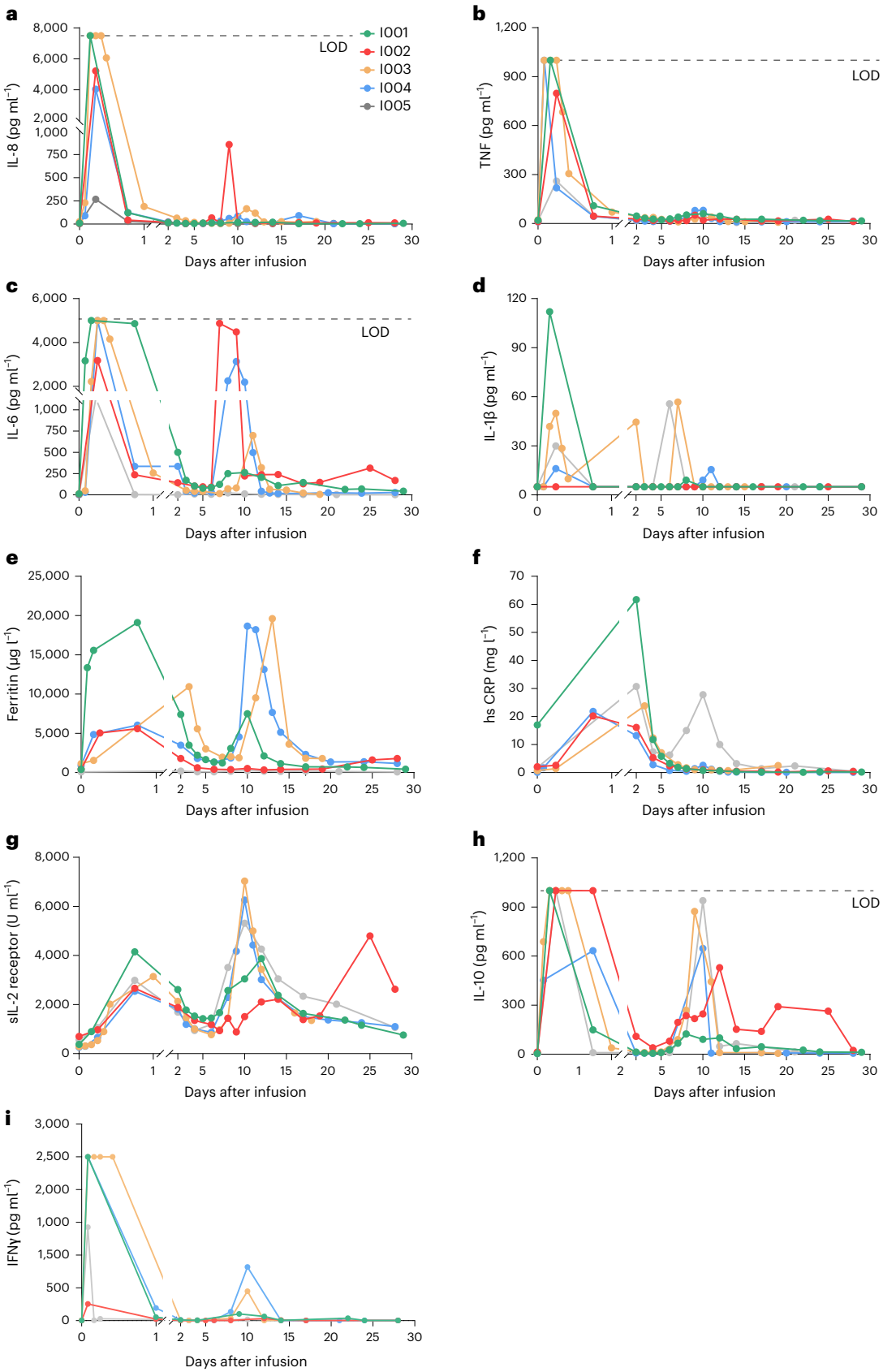

Fig. 3 | Biphasic immune toxicity responses following ESO-T01 infusion. **a**–**i**, Serum levels of IL-8 (**a**), TNF (**b**), IL-6 (**c**), IL-1β (**d**), ferritin (**e**), hs-CRP (**f**), sIL-2R (**g**), IL-10 (**h**) and IFNγ (**i**) exhibited a biphasic pattern. An early surge within 24 hours reflected acute-phase inflammation likely triggered by lentiviral vector sensing and associated with myeloid activation. A second wave, emerging between days 6 and 14, coincided with peak CAR-T expansion and was characterized by elevations in IL-6, IL-1β, IL-10, ferritin and sIL-2R, consistent with adaptive immune activation. This kinetic separation suggests a transition from vector-driven innate inflammation to CAR-T-mediated adaptive immunity. LOD, limit of detection.

https://doi.org/10.1038/s41591-026-04244-6

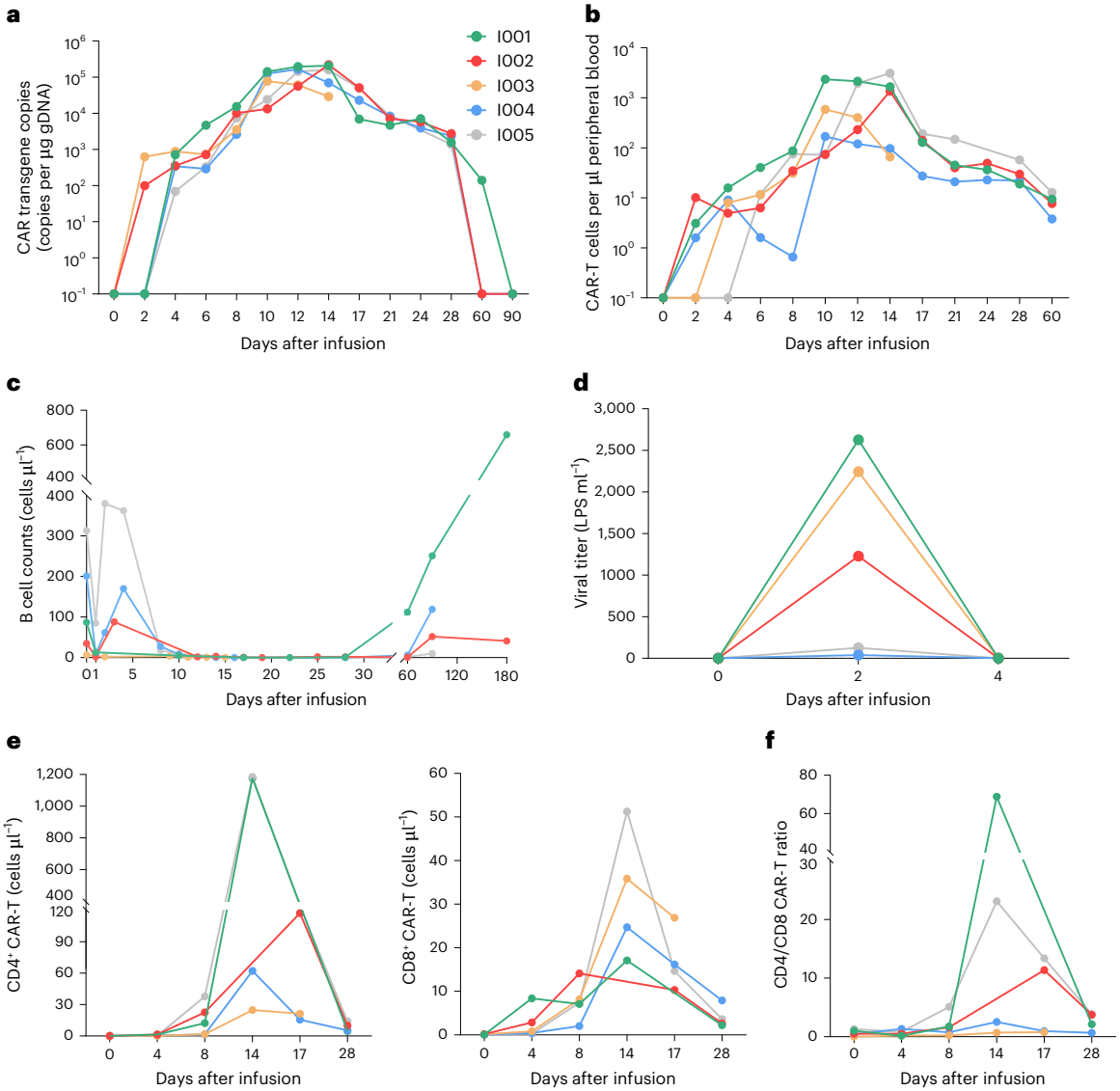

Fig. 4 | In vivo expansion kinetics and immune reconstitution of ESO-T01 CAR-T cells. a, CAR transgene copy number in peripheral blood mononuclear cells measured by qPCR, showing rapid expansion with peak levels at days 10–14 in most patients. **b**, Enumeration of circulating CAR-T cells by flow cytometry, confirming expansion kinetics consistent with qPCR. **c**, Absolute counts of CD19⁺ B cells, showing near-complete depletion by day 10, with recovery in some patients during follow-up. **d**, Viral titers in peripheral blood at early timepoints, peaking around day 2. **e**, Longitudinal profiling of CD4⁺ and CD8⁺ CAR-T subsets, with absolute counts plotted over time. **f**, CD4/CD8 CAR-T ratio during the expansion phase, illustrating a transient CD4-skewed phenotype at peak proliferation. Together, **c**, **e** and **f** depict treatment-related immune reconstitution. LPS, lipopolysaccharide.

Sensitivity analyses

No formal sensitivity analyses were conducted owing to the small sample size and early-phase design of this study.

Post hoc analyses

Following the protocol amendment, prophylactic dexamethasone (20 mg intravenously, 1 hour before infusion) was administered to the four subsequent patients. Under this modified regimen, toxicity was markedly attenuated. Two patients developed grade 3 CRS, and one patient developed grade 2 CRS; none required vasopressors. In accordance with European Society of Blood and Marrow Transplantation/European Hematology Association (EBMT/EHA) guidelines, tocilizumab was administered in three cases, with prompt resolution of symptoms[23]; one patient experienced no CRS. Most adverse events resolved either spontaneously or with treatment, and the prophylactic intervention did not impair CAR-T expansion.

Discussion

This phase 1 trial demonstrates that ESO-T01, a replication-incompetent, nanobody-directed lentiviral vector, can reliably generate CAR-T cells in vivo. A single intravenous infusion achieved robust expansion and persistence without leukapheresis, ex vivo manufacturing or lymphodepleting chemotherapy, underscoring the feasibility of this approach. In this study, the interval from enrollment to infusion was short (median, 8 hours, 37 minutes; range, 2:00–23:48), reflecting that administration could be scheduled promptly once enrollment was confirmed. The primary endpoint of safety was met: no DLTs were observed, and adverse events were manageable with supportive care.

Compared to established autologous BCMA-directed CAR-T products such as ide-cel and cilta-cel, ESO-T01 introduces several distinct features, including vector-driven innate immune activation preceding CAR-T expansion and engraftment without conditioning. Although the incidence of CRS and ICANS was consistent with prior ex vivo CAR-T experiences, the timing and sequence of toxicities suggest different

underlying biology. Notably, no unexpected or clinically meaningful off-target events were identified.

The study population represented a heavily pretreated, high-risk cohort, with a median of three prior lines of therapy and extensive exposure to proteasome inhibitors, IMiD and anti-CD38 antibodies. One patient could not receive an IMiD due to a history of lower limb thrombosis. Only one patient had previously undergone ASCT, a proportion substantially lower than that reported in Western trials. This reflects treatment patterns in China, where ASCT uptake remains limited due to accessibility and practice differences, as documented in national registry studies[24–26]. This cohort was entirely independent of the four patients reported in a previous correspondence[22], allowing distinct follow-up and baseline characterization.

ESO-T01 incorporates multiple vector engineering refinements intended to optimize selective T cell programming. These include pseudotyping to enforce T cell tropism, CD47 overexpression to reduce clearance by the mononuclear phagocyte system, removal of major histocompatibility complex class I (MHC-I) to limit immunogenicity and the addition of an anti-TCR nanobody to achieve T-cell-specific targeting[27,28]. Unlike conventional autologous CAR-T therapies, ESO-T01 enables in vivo programming with a single infusion, potentially broadening accessibility while preserving the biological fitness of engineered cells.

Most adverse events were transient cytopenias and biochemical abnormalities that resolved without sequelae. The transient cytopenias occurred primarily within approximately 2 hours of infusion, despite the absence of lymphodepleting chemotherapy. These acute cytopenias are most consistent with innate immune activation triggered by in vivo vector delivery, occurring prior to detectable CAR-T expansion. Possible mechanisms include cytokine-driven redistribution and changes in vascular permeability as well as transient hematopoietic suppression or T cell sequestration triggered by engagement of innate sensing pathways such as Toll-like receptors (TLRs) and cyclic GMP-AMP synthase (cGAS)–stimulator of interferon genes (STING)[27,29–31]. Notably, such early cytopenias have not been observed with conventional ex vivo CAR-T therapies, underscoring that this phenomenon is specific to in vivo delivery. Further studies are required to confirm the underlying mechanisms.

Sentinel cases further delineate the boundaries of safety. Patient I001 developed a hyperacute inflammatory reaction within hours of infusion, likely mediated by innate sensing rather than CAR-T expansion. This led to a protocol amendment introducing prophylactic corticosteroids, which successfully mitigated early CRS in subsequent patients without impairing CAR-T proliferation. By contrast, patient I003 developed fatal spinal cord compression temporally associated with peak expansion. Imaging suggested inflammatory edema or pseudoprogression, although true progression could not be excluded, a phenomenon recognized in other CAR-T settings[32,33]. Serological markers showed substantial declines despite radiographic worsening, highlighting the complexity of interpreting biomarker dynamics. This case underscores the importance of anatomical risk stratification in patients with extramedullary disease.

Cytokine profiling revealed a biphasic pattern distinct from ex vivo CAR-T therapy. An early 'innate wave' occurred within 24 hours, characterized by elevations in IL-6, IL-8, TNF and ferritin before CAR-T detection. A second 'adaptive wave' appeared between days 6 and 14, coinciding with expansion and marked by increases in sIL-2R, IFNγ and IL-10. IFNγ displayed a biphasic profile, supporting a transition from vector-induced innate activation to CAR-T-driven adaptive immunity[34,35]. Transient cytopenias and reversible hepatic enzyme elevations observed in this period further support a role for innate vector sensing. Notably, prophylactic corticosteroids attenuated early CRS without diminishing CAR-T expansion or antimyeloma activity[36,37], defining a therapeutic window in which toxicity and efficacy may be decoupled. In several patients, biochemical responses preceded detectable CAR-T cells, raising the possibility that innate activation contributed to early tumor debulking and microenvironment priming.

Pharmacologic data confirm the efficiency of in vivo programming. All patients received a single infusion of 0.2×10^9 transduction units, far below doses commonly required for ex vivo manufacturing or used in non-human primate studies[5,6,27]. Nevertheless, robust expansion was achieved, with CAR-T cells comprising up to 59.1% of $CD3^+$ T cells and vector copy numbers reaching 220,000 copies per microgram of gDNA. Vector copy numbers were similar to those reported for autologous BCMA CAR-T products such as ide-cel, cilta-cel and equecabtagene autoleucel[5,6,38]. Flow cytometry showed no detectable off-target transduction in $CD3^-$ subsets, supporting a favorable biosafety profile. In one patient, CAR-T cells were identified in pleural effusion, suggesting tissue penetration and trafficking. These findings support the pharmacologic efficiency of in vivo delivery while reducing vector requirements.

B cell depletion provided further insight into platform-specific biology. Despite the absence of lymphodepleting chemotherapy, all patients experienced transient B cell aplasia within 30 days. Potential mechanisms include transient BCMA upregulation on immature precursors under inflammatory conditions[39–41] or cytokine-mediated suppression of lymphopoiesis[42–44]. Between 2 months and 6 months, malignant plasma cell clearance and reduced antigenic drive were followed by reconstitution of normal B cells as CAR-T levels declined. Notably, recovery occurred alongside ongoing clinical responses, indicating that ESO-T01 retains antitumor activity despite physiological immune reconstitution.

Longitudinal immunophenotyping demonstrated that both $CD4^+$ and $CD8^+$CAR-T cells peaked around day 14, consistent with previous reports of BCMA CAR-T expansion kinetics[45,46]. Subset analysis revealed transitions from naive and effector states toward central and effector memory subsets, particularly within the $CD8^+$ compartment. PD-1 expression rose transiently early after infusion but subsequently declined and remained low, consistent with activation dynamics.

Collectively, these clinical and translational findings indicate that in vivo CAR-T therapy should be regarded not simply as a manufacturing simplification but also as a biologically distinct platform requiring tailored clinical oversight. By eliminating leukapheresis, ex vivo processing and conditioning, ESO-T01 reduces treatment delays and procedural complexity. At the same time, unique pharmacologic properties—vector-driven innate inflammation, expansion without preconditioning and endogenous differentiation trajectories—necessitate refinement of clinical monitoring. Conventional CRS and ICANS grading frameworks may not fully capture these dynamics; for example, early hypotension or fever preceding CAR-T detection may not meet grading thresholds yet still represent clinically meaningful toxicity. Future monitoring systems should incorporate innate response windows, vector-specific inflammatory profiles and anatomical risk stratification.

Limitations of this early-phase trial include the small cohort size and single-center design as well as the absence of biopsies that could have provided mechanistic insights into innate immune responses and tumor pseudoprogression. Although no evidence of clinically meaningful off-target transduction was observed, potential events in hematopoietic or other immune cells remain a concern, and long-term follow-up will be required to assess the risk of insertional mutagenesis or secondary malignancies. The durability of clinical responses is not yet defined. Future study designs may incorporate safety switches such as suicide genes, and vector refinements—including codon optimization, reduction of CpG motifs, alternative pseudotyping strategies or glycosylation shielding approaches targeting innate immune sensors such as TLR9—could mitigate innate immune activation[47–49]. In addition, dose optimization and multicenter evaluation will be necessary to establish generalizability. Taken together, these considerations outline the key priorities for future clinical development of in vivo CAR-T therapy.

In conclusion, ESO-T01 represents a promising candidate for in vivo CAR-T therapy in multiple myeloma. This early-phase trial establishes the feasibility of in vivo CAR-T generation with an acceptable and manageable safety profile. The distinct immune dynamics observed here, together with protocol-defined eligibility ensuring appropriate enrollment, provide a foundation for the rational development of this next-generation CAR-T platform.

Online content

Any methods, additional references, Nature Portfolio reporting summaries, source data, extended data, supplementary information, acknowledgements, peer review information; details of author contributions and competing interests; and statements of data and code availability are available at https://doi.org/10.1038/s41591-026-04244-6.

References

1. Kumar, S. K. et al. Multiple myeloma. *Nat. Rev. Dis. Primers* **3**, 17046 (2017).
2. Kumar, S. K. et al. Risk of progression and survival in multiple myeloma relapsing after therapy with IMiDs and bortezomib: a multicenter international myeloma working group study. *Leukemia* **26**, 149–157 (2012).
3. Cappell, K. M. & Kochenderfer, J. N. Long-term outcomes following CAR T cell therapy: what we know so far. *Nat. Rev. Clin. Oncol.* **20**, 359–371 (2023).
4. Yu, B., Jiang, T. & Liu, D. BCMA-targeted immunotherapy for multiple myeloma. *J. Hematol. Oncol.* **13**, 125 (2020).
5. Munshi, N. C. et al. Idecabtagene vicleucel in relapsed and refractory multiple myeloma. *N. Engl. J. Med.* **384**, 705–716 (2021).
6. Berdeja, J. G. et al. Ciltacabtagene autoleucel, a B-cell maturation antigen-directed chimeric antigen receptor T-cell therapy in patients with relapsed or refractory multiple myeloma (CARTITUDE-1): a phase 1b/2 open-label study. *Lancet* **398**, 314–324 (2021).
7. Wang, D. et al. A phase 1 study of a novel fully human BCMA-targeting CAR (CT103A) in patients with relapsed/refractory multiple myeloma. *Blood* **137**, 2890–2901 (2021).
8. Chen, W. et al. Phase II study of fully human BCMA-targeting CAR-T cells (zevorcabtagene autoleucel) in patients with relapsed/refractory multiple myeloma. *Exp. Hematol. Oncol.***14**, 119 (2025).
9. Locke, F. L. et al. Impact of vein-to-vein time in patients with R/R LBCL treated with axicabtagene ciloleucel. *Blood Adv.* **9**, 2663–2676 (2025).
10. Amini, L. et al. Preparing for CAR T cell therapy: patient selection, bridging therapies and lymphodepletion. *Nat. Rev. Clin. Oncol.* **19**, 342–355 (2022).
11. Ayala Ceja, M., Khericha, M., Harris, C. M., Puig-Saus, C. & Chen, Y. Y. CAR-T cell manufacturing: major process parameters and next-generation strategies. *J. Exp. Med.* **221**, e20230903 (2024).
12. Mailankody, S. et al. Allogeneic BCMA-targeting CAR T cells in relapsed/refractory multiple myeloma: phase 1 UNIVERSAL trial interim results. *Nat. Med.* **29**, 422–429 (2023).
13. Marin, D. et al. Safety, efficacy and determinants of response of allogeneic CD19-specific CAR-NK cells in CD19$^+$ B cell tumors: a phase 1/2 trial. *Nat. Med.* **30**, 772–784 (2024).
14. Heczey, A. et al. Anti-GD2 CAR-NKT cells in relapsed or refractory neuroblastoma: updated phase 1 trial interim results. *Nat. Med.* **29**, 1379–1388 (2023).
15. Diorio, C., Teachey, D. T. & Grupp, S. A. Allogeneic chimeric antigen receptor cell therapies for cancer: progress made and remaining roadblocks. *Nat. Rev. Clin. Oncol.* **22**, 10–27 (2025).
16. Labanieh, L. & Mackall, C. L. CAR immune cells: design principles, resistance and the next generation. *Nature* **614**, 635–648 (2023).
17. Hunter, T. L. et al. In vivo CAR T cell generation to treat cancer and autoimmune disease. *Science* **388**, 1311–1317 (2025).
18. Nicolai, C. J. et al. In vivo CAR T-cell generation in nonhuman primates using lentiviral vectors displaying a multidomain fusion ligand. *Blood* **144**, 977–987 (2024).
19. Nawaz, W. et al. AAV-mediated in vivo CAR gene therapy for targeting human T-cell leukemia. *Blood Cancer J.* **11**, 119 (2021).
20. Bozza, M. et al. A nonviral, nonintegrating DNA nanovector platform for the safe, rapid, and persistent manufacture of recombinant T cells. *Sci. Adv.* **7**, eabf1333 (2021).
21. Rurik, J. G. et al. CAR T cells produced in vivo to treat cardiac injury. *Science* **375**, 91–96 (2022).
22. Xu, J. et al. In-vivo B-cell maturation antigen CAR T-cell therapy for relapsed or refractory multiple myeloma. *Lancet* **406**, 228–231 (2025).
23. Yakoub-Agha, I. et al. Management of adults and children undergoing chimeric antigen receptor T-cell therapy: best practice recommendations of the European Society for Blood and Marrow Transplantation (EBMT) and the Joint Accreditation Committee of ISCT and EBMT (JACIE). *Haematologica* **105**, 297–316 (2020).
24. Fan, H. et al. Current treatment paradigm and survival outcomes among patients with newly diagnosed multiple myeloma in China: a retrospective multicenter study. *Cancer Biol. Med.* **20**, 77–87 (2023).
25. Tang, W. et al. Treatment attrition rates and relevant risk factors in multiple myeloma: a real-world study in China. *Front. Pharmacol.* **14**, 979111 (2023).
26. Cowan, A. J. et al. The global state of hematopoietic cell transplantation for multiple myeloma: an analysis of the Worldwide Network of Blood and Marrow Transplantation Database and the Global Burden of Disease Study. *Biol. Blood Marrow Transplant.* **26**, 2372–2377 (2020).
27. Milani, M. et al. Phagocytosis-shielded lentiviral vectors improve liver gene therapy in nonhuman primates. *Sci. Transl. Med.* **11**, eaav7325 (2019).
28. Milani, M. et al. Genome editing for scalable production of alloantigen-free lentiviral vectors for in vivo gene therapy. *EMBO Mol. Med.* **9**, 1558–1573 (2017).
29. Wang, Y. & Shao, W. Innate immune response to viral vectors in gene therapy. *Viruses* **15**, 1801 (2023).
30. Kim, J. T. et al. Dendritic cell–targeted lentiviral vector immunization uses pseudotransduction and DNA-mediated STING and cGAS activation. *Sci. Immunol.* **2**, eaal1329 (2017).
31. Ganaie, S. S., Wang, Z., Su, B. & Mir, S. Editorial: Virus-induced innate immune response and inflammation. *Front. Microbiol.* **14**, 1213270 (2023).
32. Huang, J., Rong, L., Wang, E. & Fang, Y. Pseudoprogression of extramedullary disease in relapsed acute lymphoblastic leukemia after CAR T-cell therapy. *Immunotherapy* **13**, 5–10 (2021).
33. Danylesko, I. et al. Immune imitation of tumor progression after anti-CD19 chimeric antigen receptor T cells treatment in aggressive B-cell lymphoma. *Bone Marrow Transplant.* **56**, 1134–1143 (2021).
34. Ivashkiv, L. B. & Donlin, L. T. Regulation of type I interferon responses. *Nat. Rev. Immunol.* **14**, 36–49 (2014).
35. Xiao, X. et al. Mechanisms of cytokine release syndrome and neurotoxicity of CAR T-cell therapy and associated prevention and management strategies. *J. Exp. Clin. Cancer Res.* **40**, 367 (2021).
36. Butman, J. et al. Steroid prophylaxis in patients receiving CAR T-cell therapy for relapsed and refractory non-Hodgkin lymphoma. *Blood* **144**, 4507–4507 (2024).
37. Costa, B. A. et al. Prognostic impact of corticosteroid and tocilizumab use following chimeric antigen receptor T-cell therapy for multiple myeloma. *Blood Cancer J.* **14**, 84 (2024).

38. Li, C. et al. Equecabtagene autoleucel in patients with relapsed or refractory multiple myeloma: the FUMANBA-1 nonrandomized clinical trial. *JAMA Oncol.* **10**, 1681–1688 (2024).
39. Dogan, A. et al. B-cell maturation antigen expression across hematologic cancers: a systematic literature review. *Blood Cancer J.* **10**, 73 (2020).
40. Kim, I., Wu, G., Chai, N., Jordan, S. & Klein, A. Dynamic BCMA expression by alloreactive B cells coupled with donor specific antibody production during de novo alloantibody responses. *J. Heart Lung Transplant.* **38**, S249 (2019).
41. Martin, J. et al. B-cell maturation antigen (BCMA) as a biomarker and potential treatment target in systemic lupus erythematosus. *Int. J. Mol. Sci.* **25**, 10845 (2024).
42. Maeda, K. et al. Interleukin-6 aborts lymphopoiesis and elevates production of myeloid cells in systemic lupus erythematosus-prone B6.*Sle1.Yaa* animals. *Blood* **113**, 4534–4540 (2009).
43. Sun, Y. et al. Early B lymphocyte subsets in blood predict prognosis in sepsis. *Front. Immunol.* **15**, 1437864 (2024).
44. Wang, X. et al. Dysregulated hematopoiesis in bone marrow marks severe COVID-19. *Cell Discov.* **7**, 60 (2021).
45. Raje, N. et al. Anti-BCMA CAR T-cell therapy bb2121 in relapsed or refractory multiple myeloma. *N. Engl. J. Med.* **380**, 1726–1737 (2019).
46. Martin, N. et al. Idecabtagene vicleucel (ide-cel, bb2121) responses are characterized by early and temporally consistent activation and expansion of CAR T cells with a T effector phenotype. *Blood* **136**, 17–18 (2020).
47. Wright, J. F. Quantification of CpG motifs in rAAV genomes: avoiding the Toll. *Mol. Ther.* **28**, 1756–1758 (2020).
48. Paremskaia, A. I. et al. Codon-optimization in gene therapy: promises, prospects and challenges. *Front. Bioeng. Biotechnol.* **12**, 1371596 (2024).
49. Yoshida, T. et al. Introduction of sugar-modified nucleotides into CpG-containing antisense oligonucleotides inhibits TLR9 activation. *Sci. Rep.* **14**, 11540 (2024).

[1]Department of Hematology, Tongji Hospital, Tongji Medical College, Huazhong University of Science and Technology, Wuhan, China. [2]Shenzhen Pregene Biopharma, Shenzhen, China. [3]EsoBiotec, Mont-Saint-Guibert, Belgium. [4]Key Laboratory of Vascular Aging, Ministry of Education, Tongji Hospital, Tongji Medical College, Huazhong University of Science and Technology, Wuhan, China. [5]Immunotherapy Research Center for Hematologic Diseases of Hubei Province, Wuhan, China. [6]These authors contributed equally: Ning An, Di Wang, Peiling Zhang, Jishuai Zhang, Philippe Parone.
✉e-mail: cunrui5650@hust.edu.cn

Methods

Study design and participants

This was a phase 1, single-arm, open-label clinical trial of ESO-T01 conducted at Tongji Hospital in Wuhan, China (ClinicalTrials.gov: NCT06791681; registered 9 January 2025; https://clinicaltrials.gov/study/NCT06791681). The trial was designed to evaluate the safety, tolerability and preliminary efficacy of ESO-T01, a replication-incompetent, TCR-targeted lentiviral vector encoding a humanized anti-BCMA CAR, delivered in vivo. The protocol was approved by the institutional review board of Tongji Medical College, Huazhong University of Science and Technology, and all participants provided written informed consent before enrollment. The study adhered to the Declaration of Helsinki, Good Clinical Practice guidelines and local regulatory requirements.

Enrollment was discontinued in early 2025 following acquisition of the original sponsor, EsoBiotec, by AstraZeneca, and the study was closed after treatment of five patients. This decision was independent of safety or efficacy considerations. These five patients constituted the final analysis set.

The clinical protocol was amended to introduce prophylactic corticosteroids (dexamethasone 20 mg intravenously, 1 hour before infusion) and to remove the single-infusion restriction for ESO-T01. Additional operational changes included adjusting enrollment intervals; clarifying the timing of urine protein electrophoresis, urine immunofixation electrophoresis and urine free light chain assessments; and modifying the study schedule, including discretionary acceptance of test results obtained within 7 days before screening as screening period data (see supplementary information for details of the protocol amendment).

Sex was determined based on self-report. Due to the limited number of eligible patients, the sex and/or gender of participants could not be specifically considered before enrollment. As the sample size was small, no disaggregated analysis by sex was conducted.

All enrolled patients received study-related medications, tests and treatments free of charge during participation. Transportation reimbursement was provided for follow-up visits.

Study eligibility

Inclusion criteria. Eligible patients were adults (≥18 years of age) of any gender with a confirmed diagnosis of multiple myeloma according to International Myeloma Working Group (IMWG) criteria[50], with BCMA expression on malignant plasma cells verified by flow cytometry or bone marrow pathology with immunohistochemistry. Patients must have received at least two prior lines of therapy (each comprising at least one full cycle) and shown disease progression within 12 months of the most recent treatment or been deemed refractory to both an immunomodulatory drug and a proteasome inhibitor, with progression documented during or within 2 months after the last therapy. Measurable disease at screening was required, defined by at least one of the following: serum M protein ≥0.5 g dl^{-1}, urine M protein ≥200 mg per 24 hours or involved serum free light chain ≥10 mg dl^{-1} with an abnormal κ/λ ratio.

Additional requirements included an Eastern Cooperative Oncology Group (ECOG) performance status of 0–2 and an expected survival of at least 3 months. Bone marrow function test results, obtained at screening or within 2 months prior to screening, were required to meet the following criteria: hemoglobin ≥6 g dl^{-1} (no red blood cell transfusions within 1 week prior to screening), and the use of recombinant human erythropoietin is allowed. For patients who meet the inclusion criterion of hemoglobin ≥6 g dl^{-1}, red blood cell transfusions are permitted to maintain hemoglobin levels at ≥6 g dl^{-1}; absolute neutrophil count ≥ 600 per microliter (without granulocyte colony-stimulating factor (G-CSF) administration within 1 week prior to screening or pegylated G-CSF within 2 weeks prior to screening); platelet count ≥ 50,000 per microliter, lymphocyte count ≥ 500 per microliter and $CD3^+$ T cell count ≥150 per microliter. Renal function had to meet creatinine clearance ≥45 ml min^{-1} (Cockcroft–Gault). Hepatic function required ALT and AST ≤ 3.0× upper limit of normal (ULN), bilirubin and alkaline phosphatase ≤ 2.0× ULN (Gilbert syndrome excepted) and albumin ≥3 g dl^{-1}. Cardiac function required left ventricular ejection fraction ≥ 40% without clinically relevant pericardial effusion or electrocardiographic abnormalities. Pulmonary function required oxygen saturation ≥ 90% without clinically relevant pleural effusion. For women of childbearing potential, a negative pregnancy test at screening and prior to infusion was mandatory; breastfeeding was not allowed. Men and women of childbearing potential were required to use effective contraception and to refrain from donating germ cells (sperm or oocytes) until 1 year after administration. Written informed consent was obtained from all participants or their legal representatives.

Exclusion criteria. Key exclusions included receipt of anticancer therapy during screening, such as targeted or epigenetic agents; participation in other interventional clinical studies or treatments involving invasive investigational medical devices within five half-lives; immune-directed or non-immune-directed systemic therapy or cytotoxic chemotherapy within 1 week; proteasome inhibitors or immunomodulatory agents within 2 weeks; or radiotherapy within 4 weeks (except when ≤5% of the bone marrow reserve was irradiated). Prior allogeneic hematopoietic stem cell transplantation within 6 months or autologous transplantation within 3 months was not permitted. Patients with active malignancies other than multiple myeloma were excluded, except those treated with curative intent and disease free ≥2 years or adequately treated non-melanoma skin cancer. Previous exposure to viruses pseudotyped with vesicular stomatitis virus glycoprotein (VSV-G) was prohibited. Additional exclusions included uncontrolled infection, active hepatitis B (HBV DNA positive), hepatitis C (HCV RNA positive), HIV, syphilis, symptomatic heart failure (New York Heart Association class III–IV), recent myocardial infarction or coronary revascularization (<6 months), clinically relevant arrhythmias, severe non-ischemic cardiomyopathy, primary immunodeficiency and stroke or seizure within 6 months before screening, dementia or altered mental status and Parkinson's disease or parkinsonism. Surgery within 2 weeks before administration or planned within 2 weeks after administration (excluding local anesthesia procedures) was not permitted. Immunization with a live attenuated vaccine within 1 month before administration was prohibited. Patients with known severe allergic reactions to ESO-T01 or its components, or to tocilizumab, were excluded. Patients unable to undergo venous access creation or those with other conditions deemed unsuitable by the investigator for study participation were also excluded.

Treatment and CAR-T cell infusion

ESO-T01 was administered as an intravenous infusion on day 0 at a fixed dose of 0.2×10^9 transduction units. The investigational product was delivered as a low-volume, slow-rate intravenous drip under continuous clinical supervision. Premedication included diphenhydramine (12.5 mg intravenously) and acetaminophen (650 mg orally), administered 1 hour before infusion.

After a sentinel case of grade 3 CRS in the first treated patient, the protocol was amended to mandate prophylactic corticosteroids. All subsequent patients received dexamethasone (20 mg intravenously, 1 hour before infusion) in addition to standard premedication.

All patients were hospitalized for infusion and remained inpatient for at least 14 days thereafter. During hospitalization, patients underwent daily monitoring including physical examination, complete blood counts, serum chemistry, coagulation profiles, cardiac and pulmonary evaluations and standardized toxicity assessments. After discharge, patients were monitored daily through day 30, either as inpatients

or during scheduled outpatient visits, with ongoing follow-up to 24 months or until study termination.

Toxicity monitoring

The primary endpoint was safety and tolerability, assessed by incidence of DLTs, treatment-emergent adverse events and laboratory abnormalities. The DLT evaluation window was defined as day 0 through day 28 after infusion. Adverse events were graded by Common Terminology Criteria for Adverse Events version 5.0 (CTCAE v5.0), and CRS and ICANS were graded according to 2019 American Society for Transplantation and Cellular Therapy (ASTCT) consensus criteria[51].

DLTs in this protocol were defined as any of the following: grade 4 or higher CRS attributed to ESO-T01; grade 3 CRS not resolving to grade 2 or lower within 7 days of onset; grade 3–4 neurotoxicity not resolving to grade 1 within 2 weeks or to baseline within 4 weeks; grade 3–5 allergic reactions attributed to ESO-T01, excluding acute infusion reactions that resolved to grade 2 or lower within 24 hours after treatment; or grade 3 or higher non-hematologic toxicities persisting beyond protocol-defined windows (72 hours for diarrhea, nausea or vomiting; 7 days for fatigue; and 14 days for hepatic or renal laboratory abnormalities).

Hematologic cytopenias were not considered DLTs. Safety monitoring included vital signs, daily hematology and chemistry panels, cardiac and pulmonary assessments and electrocardiography. Management of CRS or ICANS followed institutional algorithms, including tocilizumab and corticosteroids when indicated.

Endpoints and clinical assessments

The primary objective was to assess the safety and tolerability of ESO-T01 in patients with relapsed or refractory multiple myeloma. Safety endpoints included DLTs, adverse events, laboratory parameters, vital signs, physical examinations and electrocardiograms.

Secondary endpoints included preliminary efficacy outcomes, namely the ORR, defined as the proportion of patients achieving an sCR, complete response, VGPR or partial response, as well as TTR, DOR, PFS and overall survival.

Responses were assessed according to IMWG 2016 criteria[50]. MRD negativity was evaluated by multiparameter flow cytometry with a sensitivity threshold of 10^{-5}.

Additional secondary endpoints included pharmacokinetics (ESO-T01 expansion in peripheral blood) and pharmacodynamics (cytokine and immune biomarker profiling). Exploratory analyses included vector shedding, CAR-T cell phenotype and function, off-target detection and CAR-T cell insertion site profiling. Based on the treatment response observed in the first patient, the conditioning protocol was subsequently adjusted, and post hoc analyses were performed.

Clinical assessments were conducted at baseline and daily during hospitalization; after discharge, they were performed weekly through day 28 and subsequently per the protocol-specified schedule. Imaging studies, bone marrow evaluations and laboratory tests were obtained at protocol-defined timepoints.

Pharmacokinetics and pharmacodynamics

Pharmacokinetics. Vector copy number was quantified by qPCR at a central laboratory (Junke Zhengyuan). The assay had a validated lower limit of detection of 50 copies per microgram of gDNA. Real-time qPCR was performed on a 7500 Fast Dx Real-Time PCR System (Thermo Fisher Scientific) according to the manufacturer's instructions. The ESO-T01 transgene was detected using specific primers (forward: AGATGGCGGAGGCCTACAGT; reverse: CTGCATGTGAAGGGCGTCGT), generating a 125-bp amplicon corresponding to the CAR transgene sequence (5′-6FAM-ATTGGGATGAAAGGCGAGCGCCG-BHQ1-3′). Data acquisition and quantification were performed using 7500 Fast Dx software (Thermo Fisher Scientific) and analyzed with Microsoft Excel 2013.

Pharmacokinetic parameters included maximum observed concentration (C_{max}), time to peak expansion (T_{max}) and $AUC_{0–28\,d}$.

Pharmacodynamics. Serum cytokines, including IL-6, IL-10, IFNγ, TNF, IL-1β, IL-8 and sIL-2R, were quantified by chemiluminescence assay. Acute-phase reactants such as CRP and ferritin were also measured by immunoturbidimetry. Serum immunoglobulin isotypes (IgG, IgA and IgM) were analyzed by nephelometry.

Exploratory analyses included monitoring for ESO-T01 persistence and potential shedding in blood, urine, saliva and feces as well as evaluation of host immune responses to the vector.

Longitudinal immunophenotyping was performed to characterize ESO-T01-induced immune effects, including T cell activation (for example, CD69, CD25 and HLA-DR), functional or exhaustion markers (PD-1 and CD57) and memory differentiation subsets (naive, central memory, effector memory and effector) defined by CD45RA and CD62L. Flow cytometry samples were acquired using a DxFLEX flow cytometer (Beckman Coulter) for data collection and analysis. The selection of markers followed the study protocol and is detailed in Supplementary Fig. 5 and 6, and detailed information of flow cytometry antibodies is provided in Supplementary Table 7. CAR-T lentiviral integration sites were analyzed using the ligation-mediated PCR (LM-PCR) method performed with a PCR machine (Dongsheng) according to the manufacturer's instructions and sequenced using the Illumina NovaSeq 6000 platform (Testing Laboratory, GENEWIZ, Inc.).

CAR vector design and manufacturing

ESO-T01 is a third-generation, self-inactivating, replication-incompetent lentiviral vector engineered for in vivo T cell modification. The CAR backbone (PRG1801) (WO2025/003526A1 and CN109134665B) consists of an anti-BCMA nanobody (VHH) for antigen recognition, a CD8 hinge and transmembrane domain for structural stability, a 4-1BB co-stimulatory domain and a CD3ζ signaling domain, all under the control of a synthetic T-cell-specific promoter (SYN).

To enhance T cell selectivity and reduce off-target effects, ESO-T01 incorporates additional modifications, including a mutant VSV-G envelope, CD47 overexpression, MHC-I knockout and an anti-TCR nanobody. The underlying mechanisms and construct architecture are illustrated in Extended Data Fig. 9.

Manufacturing was performed under Good Manufacturing Practice conditions. ESO-T01 was generated by transient transfection of engineered producer 293T cells (MHC-I^-/$CD47^{hi}$/TCR-VHH^+ background) using a four-plasmid system (Gag/Pol, Rev, Env and transfer plasmid encoding PRG1801). Viral harvests were clarified, concentrated by tangential flow filtration and purified by anion-exchange chromatography, followed by sterile filtration and aseptic filling.

Final release criteria included sterility, potency, purity and vector identity. All batches were stored at ≤ −65 °C until administration.

Statistical analysis

All statistical analyses were performed according to the prespecified plan outlined in section 9 of the study protocol (version 1.1). Clinical data were collected using a validated electronic data capture system. Given the limited sample size ($n = 5$), analyses were descriptive in nature. Categorical variables were summarized as counts and percentages, and continuous variables were reported as medians with ranges.

Time-to-event outcomes, including PFS and overall survival, were estimated using the Kaplan–Meier method, with censoring at the date of last follow-up. Safety data are presented as the maximum toxicity grade per patient. Adverse events were coded using MedDRA terminology and graded by CTCAE v5.0 or by ASTCT consensus criteria for CRS and ICANS.

Because the trial was terminated early after five patients had been treated, no formal hypothesis testing, power calculation or inferential statistical analysis was performed. No statistical methods were used to

predetermine the sample size; no data were excluded from the analyses; and the study was not randomized. Prespecified statistical methods were outlined in the study protocol and the statistical analysis plan, which were approved by the institutional review board prior to patient enrollment. All analyses were performed using commercially available software packages, including FlowJo (version 10.8.1), NovoExpress, CytExpert (version 2.0) and GraphPad Prism (version 9.5.0).

Reporting summary

Further information on research design is available in the Nature Portfolio Reporting Summary linked to this article.

Data availability

All primary data supporting the findings of this study are included in this article and its supplementary files. Extended data tables and figures, together with the supplementary information, provide patient-level data for safety, response, pharmacokinetic and immunophenotyping analyses as well as vector construct, integration site analyses and gating strategies.

The clinical datasets generated and analyzed during this study are not publicly available due to proprietary restrictions and to protect patient privacy and sensitive information. All individual-level clinical data have been deidentified and are stored on the secure data server of Tongji Hospital. Interested researchers may contact the corresponding author to request access to the datasets. Access requires completion of a data access agreement describing the intended research use; commercial or for-profit use is prohibited. After approval by the applicant's institution and our institutional data access committee, deidentified individual participant-level data will be provided within 6 months after publication and will remain accessible for at least 5 years. The full trial protocol and the statistical analysis plan are provided in the supplementary materials.

All requests for data access should be directed to the corresponding author (cunrui5650@hust.edu.cn), and responses will be provided within 10 working days.

References

50. Kumar, S. et al. International Myeloma Working Group consensus criteria for response and minimal residual disease assessment in multiple myeloma. *Lancet Oncol.* **17**, e328–e346 (2016).
51. Lee, D. W. et al. ASTCT consensus grading for cytokine release syndrome and neurologic toxicity associated with immune effector cells. *Biol. Blood Marrow Transplant.* **25**, 625–638 (2019).

Acknowledgements

This work was supported by the National Natural Science Foundation of China (82170223 to C.L.) and the Natural Science Foundation of Hubei Province (2024AFD421 to C.L.). We thank H. Mei for helpful discussions. We thank all clinical investigators, research nurses and study coordinators for their contributions. We also acknowledge the members of the independent data monitoring committee for their oversight. The study was supported in part by EsoBiotec, which provided the ESO-T01 vector and technical input. The funder had no role in study design, data collection, data analysis, data interpretation or writing of the report.

Author contributions

C.L., N.A., D.W. and P.Z. contributed to the analyses and interpretation of the clinical data. J.Z. and P.P. contributed to the development of the ESO-T01 construct. C.L., D.W., P.Z. and J.Z. designed the clinical protocol. C.L., D.W., P.Z., L.X., H.R. and Y.W. contributed to the clinical treatments. N.A., J.H., X.W. and Y.G. collected and assembled data. N.A., C.L, P.Z. and Y.B. wrote the paper. C.L. directed the study and had final responsibility to submit for publication. All authors read and approved the final paper.

Competing interests

P.P. is employed by and owns stocks in EsoBiotec. J.Z. is employed by and owns stocks in Shenzhen Pregene Biopharma Company. The other authors declare no competing interests.

Additional information

Extended data is available for this paper at https://doi.org/10.1038/s41591-026-04244-6.

Supplementary information The online version contains supplementary material available at https://doi.org/10.1038/s41591-026-04244-6.

Correspondence and requests for materials should be addressed to Chunrui Li.

Peer review information *Nature Medicine* thanks Leo Rasche, Eric Smith and the other, anonymous, reviewer(s) for their contribution to the peer review of this work. Primary Handling Editor: Anna Ranzoni, in collaboration with the *Nature Medicine* team.

https://doi.org/10.1038/s41591-026-04244-6

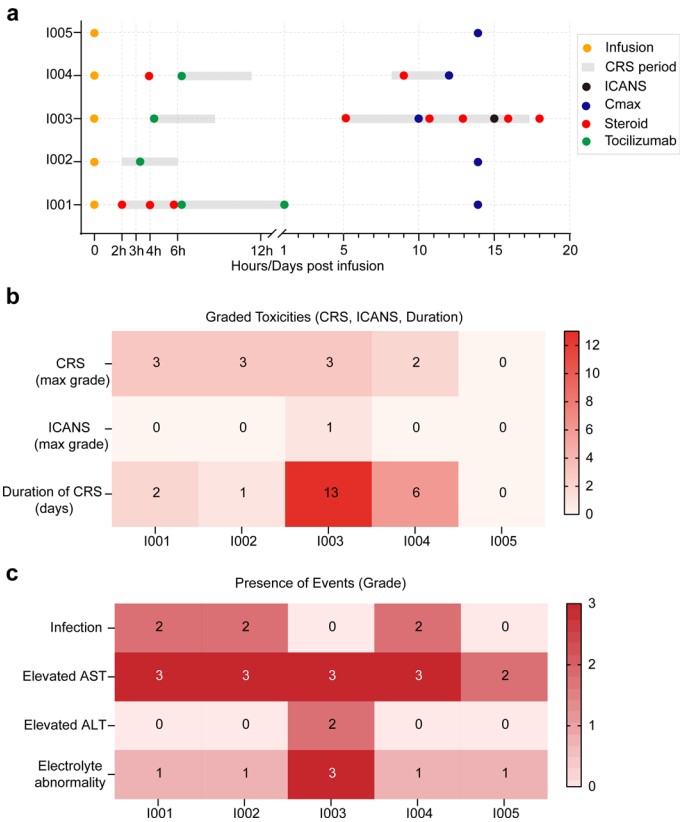

Extended Data Fig. 1 | Clinical timelines, toxicity profiles and interventions in patients treated with ESO-T01. a, Timelines illustrating infusion, CRS onset and duration, ICANS, administration of corticosteroids or tocilizumab, and the time of peak CAR-T expansion (Cmax). **b**, Maximum CRS and ICANS grades according to ASTCT criteria, together with the duration of CRS (days) in each patient. **c**, Summary of adverse events in the cohort, including infections, elevated AST/ALT and electrolyte abnormalities. Heatmap intensity indicates the maximum recorded grade for each event. Abbreviations: ALT, alanine aminotransferase; AST, aspartate aminotransferase; Cmax, maximum CAR-T cell concentration; CRS, cytokine release syndrome; ICANS, immune effector cell-associated neurotoxicity syndrome.

https://doi.org/10.1038/s41591-026-04244-6

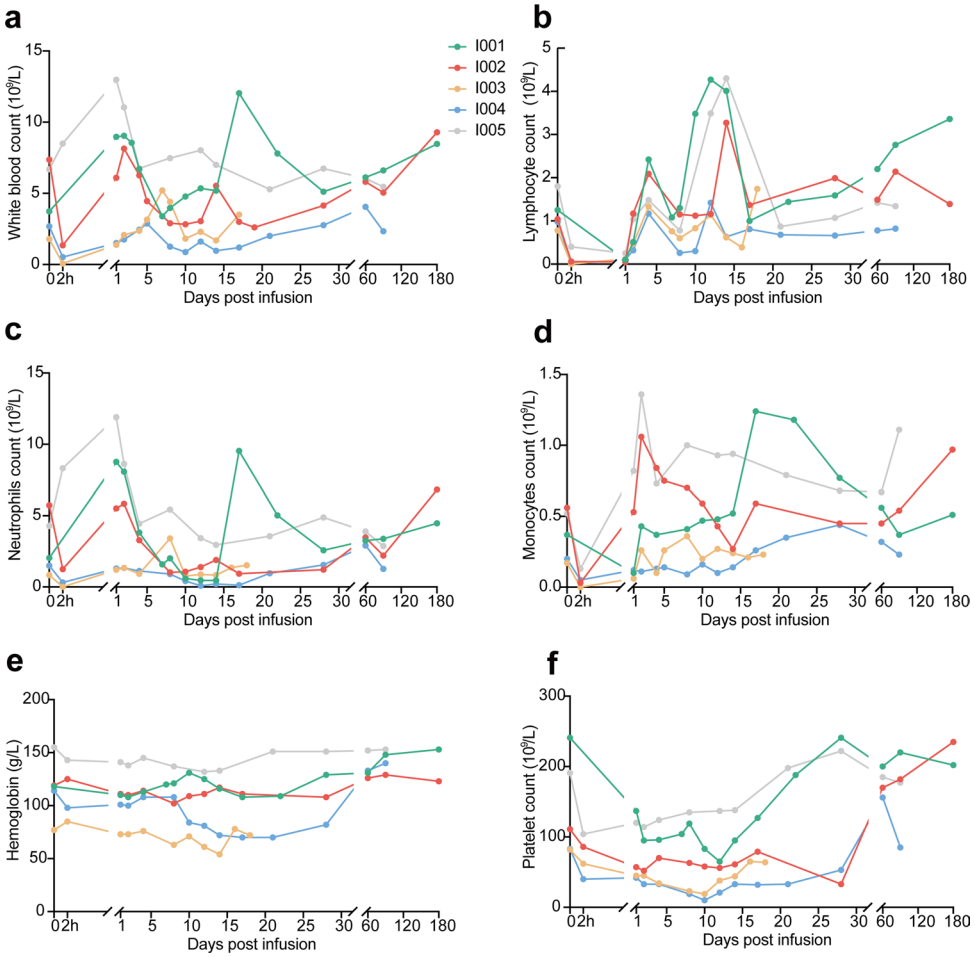

Extended Data Fig. 2 | Longitudinal changes in peripheral blood counts after ESO-T01 infusion. a, White blood cells declined within 24 hours post-infusion, followed by variable recovery profiles. **b**, Lymphocyte counts decreased rapidly and recovered to near-baseline levels over time. **c**, Neutrophil counts showed early depletion with delayed reconstitution. **d**, Monocyte counts declined acutely but demonstrated partial recovery. **e**, Hemoglobin levels reached nadirs around Days 10–15 and gradually recovered. **f**, Platelet counts similarly dropped around Days 10–15, followed by hematologic recovery over 60–120 days. Values represent absolute counts in peripheral blood.

https://doi.org/10.1038/s41591-026-04244-6

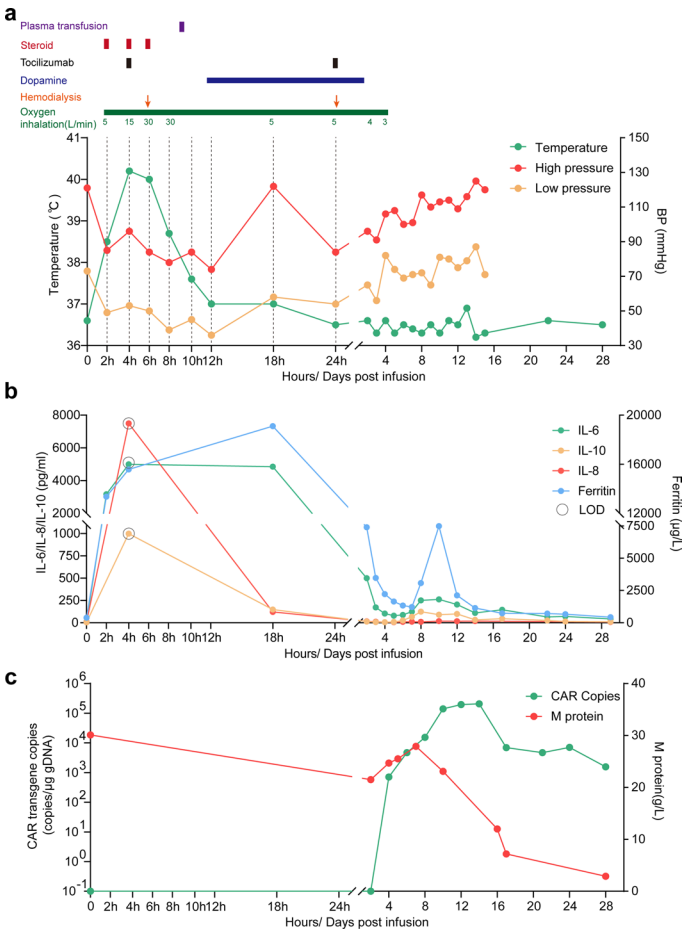

Extended Data Fig. 3 | Clinical trajectory, inflammatory markers, and CAR-T expansion in patient I001 following ESO-T01 infusion. a, Temporal changes in body temperature and blood pressure with concurrent clinical interventions. The patient developed grade 3 CRS within 2 hours of infusion, presenting with fever, hypotension, hypoxemia, and tachycardia. Management consisted of high-dose corticosteroids, tocilizumab, renal replacement therapy, dopamine, and high-flow oxygen delivered in a hematology ward equipped for ICU-level monitoring. Oxygen flow rates (L/min) are annotated along the horizontal bar. **b**, Serum cytokines (IL-6, IL-8, IL-10) and ferritin showed a hyperacute surge coinciding with CRS onset, followed by a decline after supportive therapy. **c**, Circulating CAR transgene copies became detectable after Day 4, while serum IgG-κ M protein showed a transient decline, interpreted as an immune-related fluctuation rather than tumor lysis.Abbreviations: CAR, chimeric antigen receptor; CRS, cytokine release syndrome; IL-6, interleukin-6; IL-8, interleukin-8; IL-10, interleukin-10; LOD, limit of detection.

https://doi.org/10.1038/s41591-026-04244-6

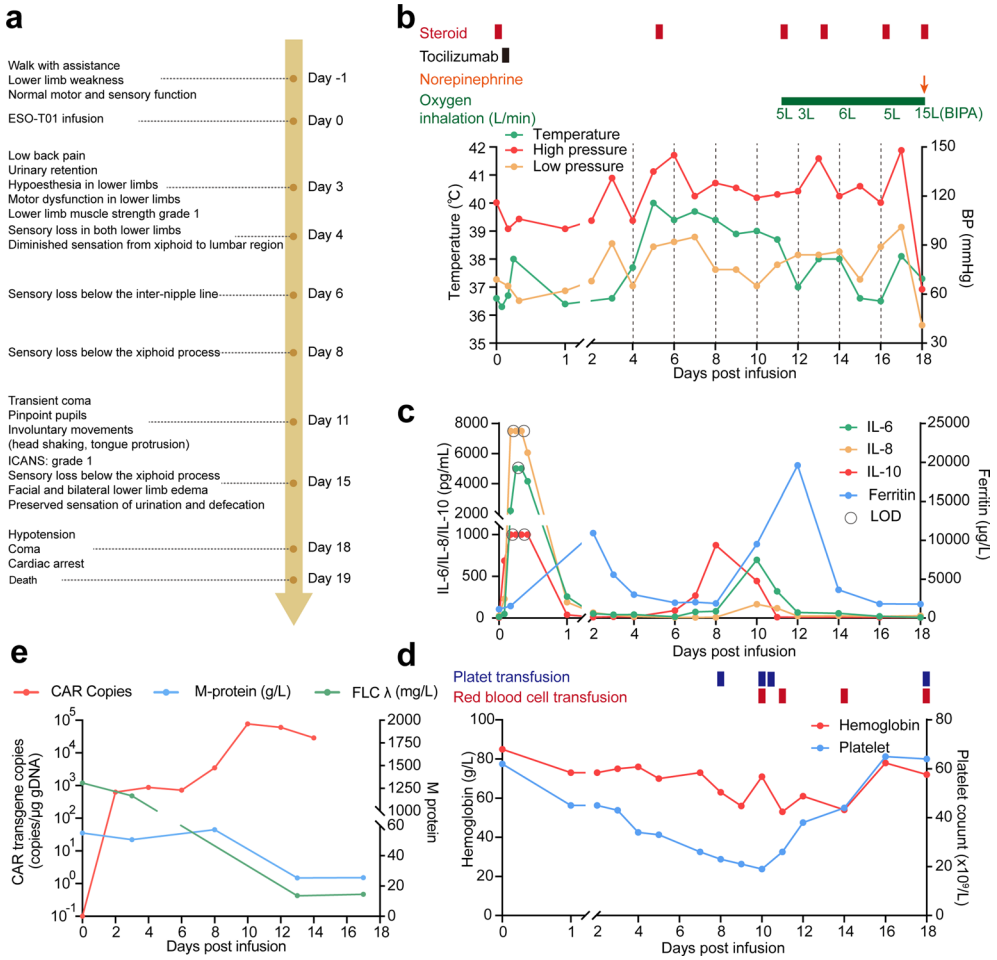

Extended Data Fig. 4 | Clinical and immunologic profile of patient I003 following ESO-T01 infusion. a, Clinical timeline from Day −1 to Day 19, showing neurologic symptoms and disease progression. The patient developed grade 3 CRS and grade 1 ICANS, ultimately progressing to cardiac arrest and death on Day 19. **b**, Daily monitoring of temperature and blood pressure, with annotations for corticosteroids (red), tocilizumab (black), norepinephrine (orange), and oxygen support (green; including bi-level positive airway pressure [BIPAP]). **c**, Serum cytokines (IL-6, IL-8, IL-10) and ferritin showed a biphasic inflammatory profile, with peaks corresponding to CRS episodes. **d**, Hemoglobin and platelet counts declined, necessitating repeated red blood cell (dark red) and platelet (dark blue) transfusions. **e**, CAR transgene copies expanded transiently in peripheral blood, accompanied by declines in M protein and FLC λ. These changes may represent transient antitumor activity or immune-related fluctuations, but no durable clinical remission was achieved. Abbreviations: BIPAP, bi-level positive airway pressure; BP, blood pressure; CAR, chimeric antigen receptor; CRS, cytokine release syndrome; FLC, free light chain; ICANS, immune effector cell-associated neurotoxicity syndrome; IL-6, interleukin-6; IL-8, interleukin-8; IL-10, interleukin-10; LOD, limit of detection.

https://doi.org/10.1038/s41591-026-04244-6

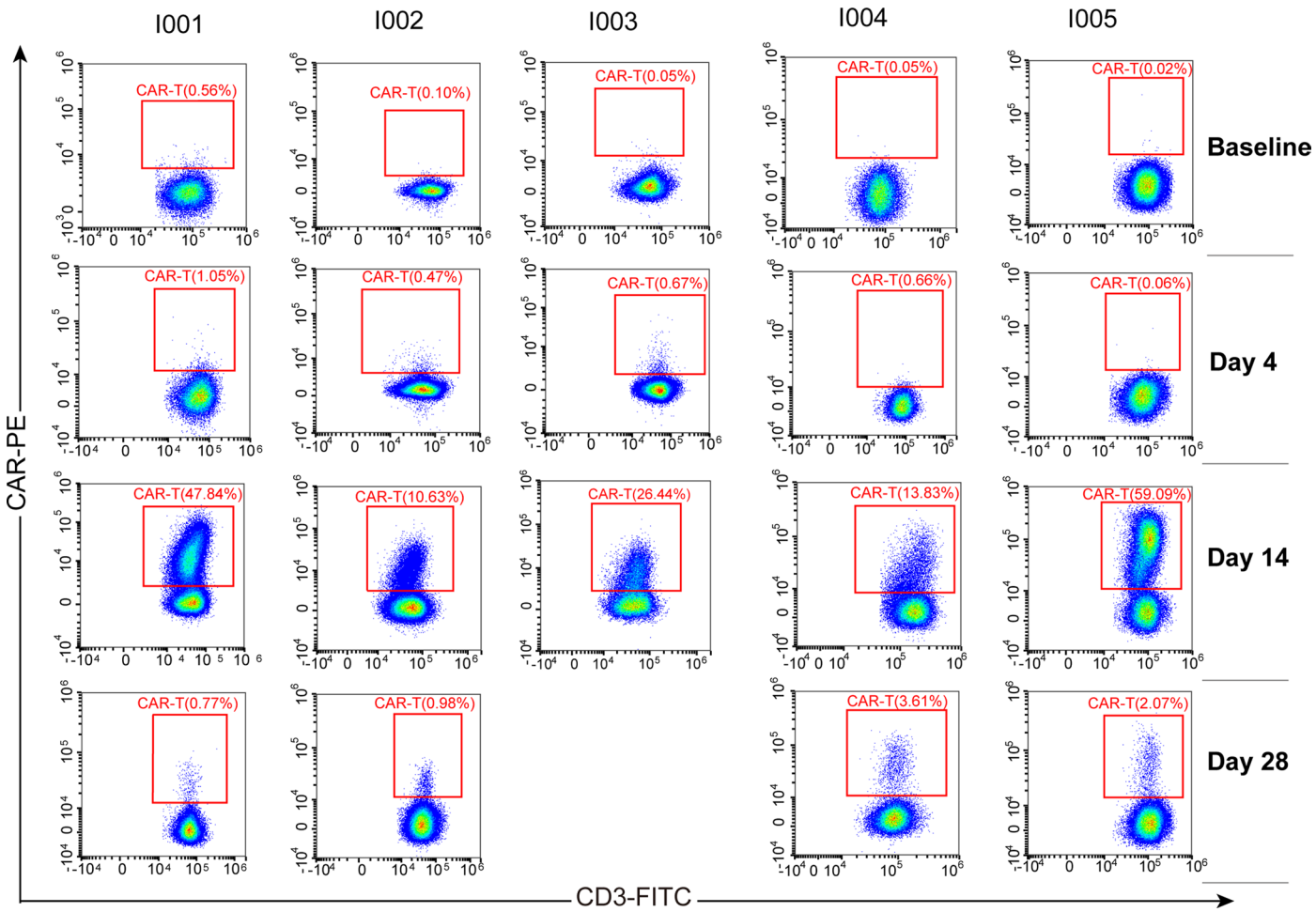

Extended Data Fig. 5 | Flow cytometry analysis of CAR-T cell expansion in peripheral blood. Representative dot plots show CAR-T cell frequencies at baseline (pre-infusion) and on days 4, 14, and 28 after infusion for each patient (I001–I005). CAR-T cells were defined as $CD3^+$ T cells co-expressing the CAR construct, detected using a PE-labeled anti-CAR antibody. Frequencies are expressed as percentages of total $CD3^+$ T cells. Expansion peaked around day 14 in most patients and declined by day 28, consistent with transient in vivo CAR-T kinetics. Abbreviations: CAR-T, chimeric antigen receptor T cell.

https://doi.org/10.1038/s41591-026-04244-6

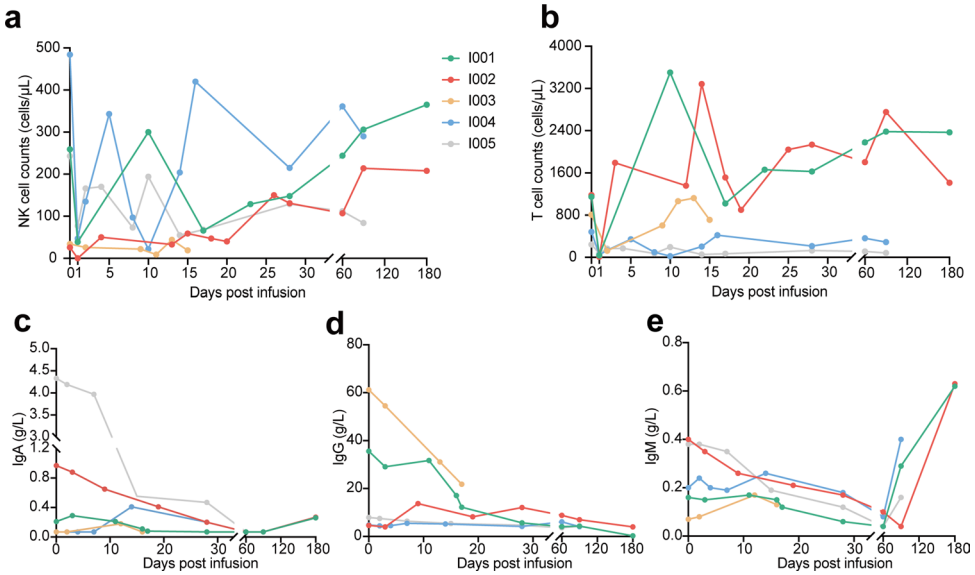

Extended Data Fig. 6 | Immune reconstitution following ESO-T01 infusion. **a**, Absolute counts of NK cells over time. **b**, Absolute counts of T cells over time. **c**–**e**, Serum immunoglobulin levels, including IgA (**c**), IgG (**d**), and IgM (**e**), declined after infusion and remained suppressed during follow-up. Together, these findings illustrate treatment-related immune reconstitution after ESO-T01 infusion. Abbreviations: Ig, immunoglobulin; NK, natural killer.

https://doi.org/10.1038/s41591-026-04244-6

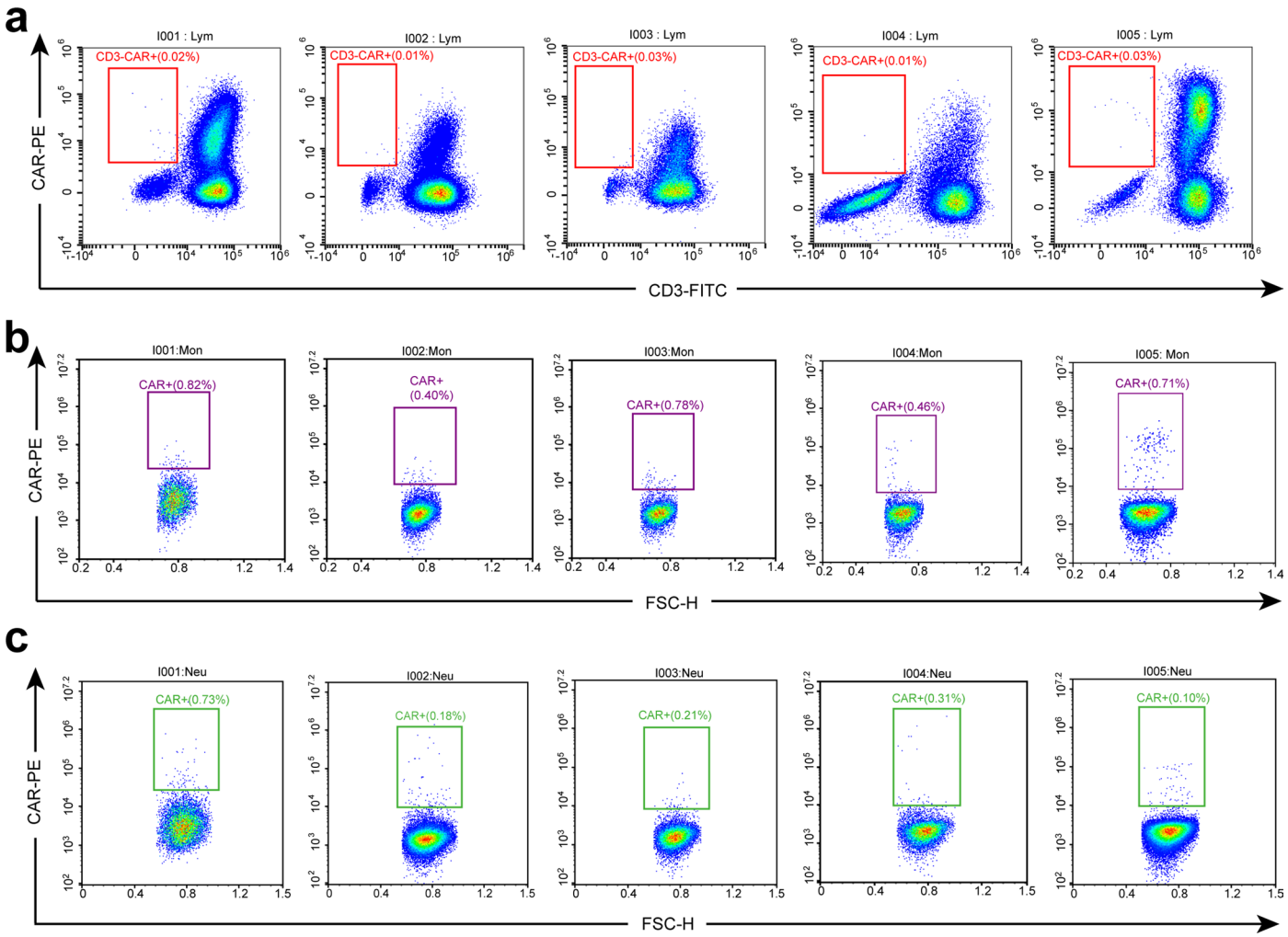

Extended Data Fig. 7 | Flow cytometry analysis of off-target transduction in patient peripheral blood at the peak of CAR-T expansion. a-c, Representative dot plots from patients I001–I005 show CAR expression within $CD3^-$ lymphocyte subsets **(a)**, monocyte subsets **(b)** and neutrophil subsets **(c)** at the time of maximal CAR-T expansion. Across all patients, the frequency of CAR^+ non-T cells remained below 1%, with CAR signal undetectable in most samples, indicating minimal off-target transduction. These data support the in vivo T-cell specificity of the ESO-T01 vector. Abbreviations: CAR, chimeric antigen receptor; CD3, cluster of differentiation 3; Lym, lymphocyte; Mon, monocyte; Neu, neutrophils.

https://doi.org/10.1038/s41591-026-04244-6

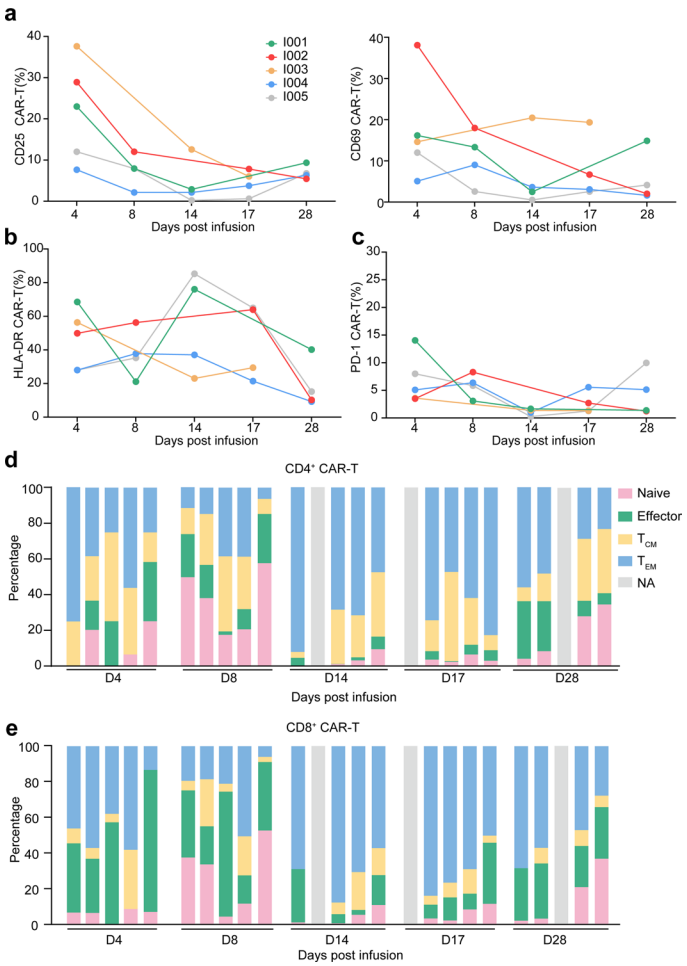

Extended Data Fig. 8 | Functional activation and phenotypic dynamics of CAR-T cells after ESO-T01 infusion. a, Temporal changes in the percentage of CD25 and CD69 CAR-T cells in peripheral blood between Days 4 and 28 post-infusion. CD25 (IL-2Rα) and CD69 are markers of early T-cell activation. **b**, Longitudinal expression of HLA-DR on CAR-T cells, associated with immune activation, with some patients showing sustained expression. **c**, PD-1 expression on CAR-T cells across multiple timepoints. A transient increase was observed shortly after infusion, which declined by Day 30, suggesting activation-related dynamics but not sufficient alone to define exhaustion. **d**, Phenotypic distribution of CD4⁺ CAR-T cells at Days 4, 8, 14, 17, and 28, classified into naïve, effector, central memory (T_{CM}), and effector memory (T_{EM}) subsets. A progressive shift toward memory phenotypes was observed. Each bar at a given time point represents data from an individual patient. **e**, Distribution of CD8⁺ CAR-T subsets across the same timepoints, showing a similar effector-to-memory transition with early expansion followed by phenotypic diversification. Each bar at a given time point represents data from an individual patient.Grey bars (NA) indicate unavailable data. Abbreviations: CD25, interleukin-2 receptor α; CD69, early T-cell activation marker; HLA-DR, human leukocyte antigen–DR; PD-1, programmed cell death protein 1; T_{CM}, central memory T cell; T_{EM}, effector memory T cell; NA, not available.

https://doi.org/10.1038/s41591-026-04244-6

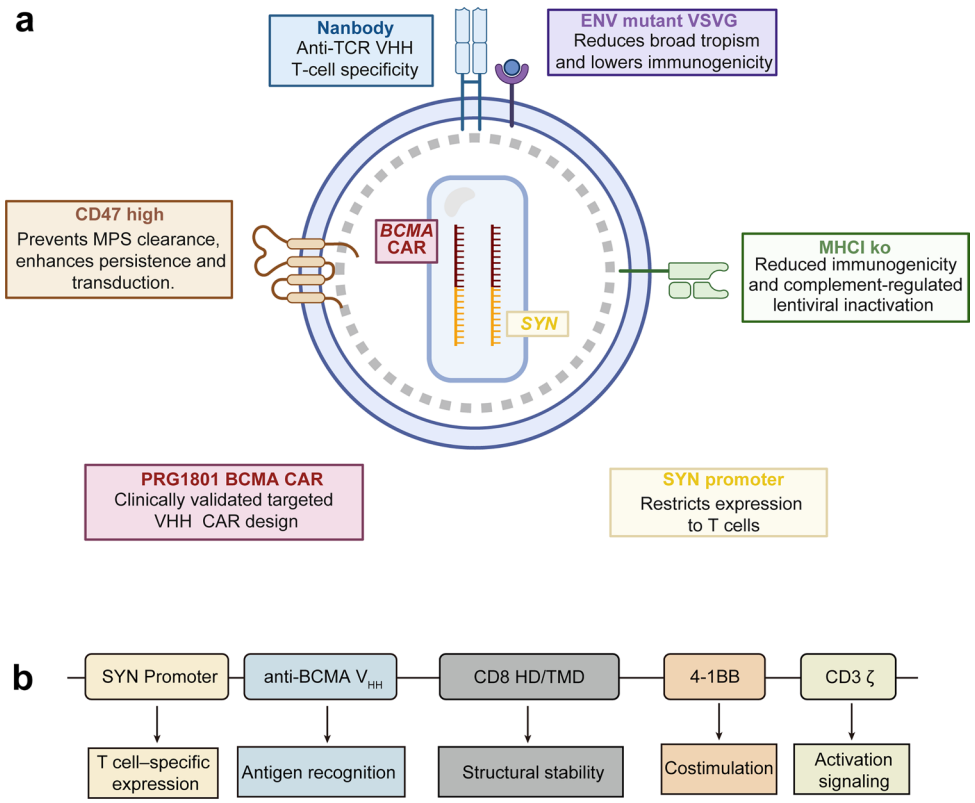

Extended Data Fig. 9 | Vector design and CAR construct of ESO-T01. a, Vector design features of ESO-T01. An anti-TCR nanobody (VHH) targets the TCR/CD3 complex to confer T-cell specificity. A mutant VSVG (ENV) envelope reduces broad tropism and lowers immunogenicity. High CD47 expression decreases clearance by the mononuclear phagocyte system, enhancing persistence and transduction. Knockout of MHC class I reduces immunogenicity and susceptibility to complement- or antibody-mediated inactivation. A synthetic T cell–specific promoter (*SYN*) restricts expression to T cells, while the BCMA CAR backbone is derived from the clinically validated PRG1801 second-generation VHH CAR. **b**, CAR construct of ESO-T01. The CAR contains an anti-BCMA VHH for antigen recognition, a CD8 hinge and transmembrane domain (TMD) for structural stability, the 4-1BB costimulatory domain, and the CD3ζ signaling domain for T-cell activation. Abbreviations: CAR, chimeric antigen receptor; BCMA, B Cell Maturation Antigen; MHC, Major Histocompatibility Complex; SYN, Synthetic T cell-specific Promoter; TCR, T Cell Receptor; VHH, Variable Domain of Heavy-chain Antibodies; VSVG, Vesicular Stomatitis Virus Glycoprotein.

https://doi.org/10.1038/s41591-026-04244-6

Extended Data Table 1 | Peak expansion, exposure kinetics, MRD status, and clinical responses of ESO-T01–generated CAR-T cells

Metric	I001	I002	I003	I004	I005
CAR-T peak (copies/µg gDNA)	207,000	220,000	77,000	166,000	157,000
$AUC_{0–28d}$ (copies·day/µg gDNA)	1,301,584	938,659	315,456	888,618	929,257
MRD status	Negative	Negative	NA	Negative	Negative
Response on Day 28	VGPR	CR	NA	PR	PR
Best response	VGPR	sCR	NE	sCR	sCR

CAR-T expansion was quantified by qPCR at serial timepoints after infusion. Peak levels and total exposure (area under the curve, AUC) from day 0 to day 28 were calculated. Minimal residual disease (MRD) was assessed by multiparameter flow cytometry, and clinical responses were evaluated according to International Myeloma Working Group (IMWG) consensus criteria. Abbreviations: AUC, area under the curve; CAR, chimeric antigen receptor; CR, complete response; IMWG, International Myeloma Working Group; MRD, minimal residual disease; NA, not applicable; NE, not estimable; PR, partial response; qPCR, quantitative polymerase chain reaction; sCR, stringent complete response; VGPR, very good partial response.

nature portfolio

Corresponding author(s): Chunrui Li

Last updated by author(s): Dec 25, 2025

Reporting Summary

Nature Portfolio wishes to improve the reproducibility of the work that we publish. This form provides structure for consistency and transparency in reporting. For further information on Nature Portfolio policies, see our Editorial Policies and the Editorial Policy Checklist.

Statistics

For all statistical analyses, confirm that the following items are present in the figure legend, table legend, main text, or Methods section.

n/a	Confirmed
☐	☒ The exact sample size (*n*) for each experimental group/condition, given as a discrete number and unit of measurement
☒	☐ A statement on whether measurements were taken from distinct samples or whether the same sample was measured repeatedly
☒	☐ The statistical test(s) used AND whether they are one- or two-sided *Only common tests should be described solely by name; describe more complex techniques in the Methods section.*
☐	☒ A description of all covariates tested
☒	☐ A description of any assumptions or corrections, such as tests of normality and adjustment for multiple comparisons
☐	☒ A full description of the statistical parameters including central tendency (e.g. means) or other basic estimates (e.g. regression coefficient) AND variation (e.g. standard deviation) or associated estimates of uncertainty (e.g. confidence intervals)
☒	☐ For null hypothesis testing, the test statistic (e.g. *F*, *t*, *r*) with confidence intervals, effect sizes, degrees of freedom and *P* value noted *Give P values as exact values whenever suitable.*
☒	☐ For Bayesian analysis, information on the choice of priors and Markov chain Monte Carlo settings
☒	☐ For hierarchical and complex designs, identification of the appropriate level for tests and full reporting of outcomes
☒	☐ Estimates of effect sizes (e.g. Cohen's *d*, Pearson's *r*), indicating how they were calculated

Our web collection on statistics for biologists contains articles on many of the points above.

Software and code

Policy information about availability of computer code

Data collection	CytoFLEX DxFLEX
Data analysis	GraphPad Prism (v9.5.0); FlowJo (v10.8.1); NovoExpress ; CytExpert (v2.0);7500 Fast DX software (Thermo Fisher Scientific);Microsoft Excel 2013

For manuscripts utilizing custom algorithms or software that are central to the research but not yet described in published literature, software must be made available to editors and reviewers. We strongly encourage code deposition in a community repository (e.g. GitHub). See the Nature Portfolio guidelines for submitting code & software for further information.

Data

Policy information about availability of data

All manuscripts must include a data availability statement. This statement should provide the following information, where applicable:

- Accession codes, unique identifiers, or web links for publicly available datasets
- A description of any restrictions on data availability
- For clinical datasets or third party data, please ensure that the statement adheres to our policy

All primary data supporting the findings of this study are included in this article and its supplementary files. Extended Data tables and figures, together with Supplementary Information, provide patient-level data for safety, response, pharmacokinetic and immunophenotyping analyses, as well as vector construct, integration-site analyses and gating strategies.

The datasets used and/or analyzed for this publication are not publicly available due to proprietary considerations and to protect the patients and their sensitive data. All individual-level clinical data have been de-identified and are stored on the secure data server of Tongji Hospital. These datasets will be made available by the corresponding author upon reasonable request within six months after publication and will remain accessible for at least five years. Requests will be reviewed by the institutional data access committee to ensure compliance with patient consent and relevant regulations, and data will be shared under an appropriate data transfer agreement when applicable. The trial protocol and statistical analysis plan can be found in the Supplementary Materials.
All requests for data access should be directed to the corresponding author (cunrui5650@hust.edu.cn), and responses will be provided within 10 working days.

Research involving human participants, their data, or biological material

Policy information about studies with human participants or human data. See also policy information about sex, gender (identity/presentation), and sexual orientation and race, ethnicity and racism.

Reporting on sex and gender	All patients signed informed consent before the start of the screening procedure. Male and female individuals aged 18 years and older were eligible to participate in the study. Sex or gender information was collected based on self-report and recorded in the electronic case report form (eCRF). The study objectives were designed independently of sex or gender. Therefore, this information was not used in the data analysis
Reporting on race, ethnicity, or other socially relevant groupings	None of these categorical variables were used.
Population characteristics	Baselines demographics and disease characteristics are summarized in Table 1. The median age of patients was 52 years (range, 52–68 years), and all five participants were male (100%). Patients had received a median of three prior lines of therapy (range, 3–5), one patient (I003) could not receive an Immunomodulatory Imide Drug (IMiD) due to a history of lower-limb thrombosis; three (60%) patients had previously been exposed to an anti-CD38 monoclonal antibody, and one (20%) had undergone autologous stem-cell transplantation (Supplementary Table 1).
Recruitment	Participants were identified by the direct medical team as part of routine clinical practice, as well as through a review of medical records and clinical databases maintained within the institution. The study included eligible participants who were adults (≥18 years) with measurable relapsed/refractory multiple myeloma (R/R MM) who had received at least two prior lines of therapy or were considered dual-refractory to both an immunomodulatory agent and a proteasome inhibitor. The full inclusion and exclusion criteria are listed in the study protocol and in the "Study eligibility" section of the methods.
Ethics oversight	The protocol was approved by the Institutional Review Board (IRB) of Tongji Medical College, Huazhong University of Science and Technology, and all participants provided written informed consent before enrollment. The study adhered to the Declaration of Helsinki, Good Clinical Practice guidelines and local regulatory requirements.

Note that full information on the approval of the study protocol must also be provided in the manuscript.

Field-specific reporting

Please select the one below that is the best fit for your research. If you are not sure, read the appropriate sections before making your selection.

☒ Life sciences ☐ Behavioural & social sciences ☐ Ecological, evolutionary & environmental sciences

For a reference copy of the document with all sections, see nature.com/documents/nr-reporting-summary-flat.pdf

Life sciences study design

All studies must disclose on these points even when the disclosure is negative.

Sample size	The sample size for this study was 5 patients with relapsed and refractory multiple myeloma. The sample size was not pre-calculated using statistical methods, as this study is a Phase 1 clinical trial with the primary aim of evaluating the safety of ESO-T01.
Data exclusions	This is a Phase 1, single-arm, prospective study. The primary, secondary, and exploratory research objectives have all been reported, and no data were excluded.
Replication	This study is a single-center Phase 1 clinical trial, with the primary objective of evaluating the safety of ESO-T01. As such, no applicable replication validation is provided.
Randomization	As this study is a single-arm design, all patients received the same treatment regimen, and therefore, random allocation was not applicable.
Blinding	This study is an open-label trial, and therefore, blinding was not implemented. All participants were aware of the treatment they received, and the researchers did not apply blinding to the treatment allocation.

Reporting for specific materials, systems and methods

We require information from authors about some types of materials, experimental systems and methods used in many studies. Here, indicate whether each material, system or method listed is relevant to your study. If you are not sure if a list item applies to your research, read the appropriate section before selecting a response.

Materials & experimental systems

n/a	Involved in the study
☐	☒ Antibodies
☒	☐ Eukaryotic cell lines
☒	☐ Palaeontology and archaeology
☒	☐ Animals and other organisms
☐	☒ Clinical data
☒	☐ Dual use research of concern
☒	☐ Plants

Methods

n/a	Involved in the study
☒	☐ ChIP-seq
☐	☒ Flow cytometry
☐	☒ MRI-based neuroimaging

Antibodies

Antibodies used: For a list of antibodies used, please refer to Supplementary Table 7

Validation: All antibodies used for flow cytometry have been validated for flow cytometry applications, and the corresponding validation flow plots are available on the manufacturer's website.

Clinical data

Policy information about clinical studies

All manuscripts should comply with the ICMJE guidelines for publication of clinical research and a completed CONSORT checklist must be included with all submissions.

Clinical trial registration: NCT06791681

Study protocol: The complete clinical study protocol has been uploaded as an attachment to the article.

Data collection: Between January and March 2025, six adults with relapsed or refractory multiple myeloma (R/R MM) were screened for eligibility. One individual did not meet the inclusion criteria and was excluded, resulting in a final cohort of five patients. Five patients received a single intravenous infusion of ESO-T01 at a dose of 0.2 × 10^9 transduction units at Tongji Hospital, Tongji Medical College, Huazhong University of Science and Technology. Clinical data were collected using an electronic data capture (EDC) system. The follow-up period ended on August 25, 2025.

Outcomes: The primary objective was to assess the safety and tolerability of ESO-T01 in patients with relapsed or refractory MM. Safety endpoints included dose-limiting toxicities (DLTs), adverse events (AEs), laboratory parameters, vital signs, physical examinations, and electrocardiograms. DLTs were assessed and the maximum tolerated dose (MTD) was determined. Adverse events were summarized by incidence, severity, and attribution, coded with MedDRA, and graded using CTCAE v5.0; Cytokine release syndrome (CRS) and immune effector cell-associated neurotoxicity syndrome (ICANS) were graded according to the 2019 ASTCT consensus criteria50. Secondary objectives were to evaluate preliminary efficacy (time to response, objective response rate [ORR], duration of response [DOR], progression-free survival [PFS], and overall survival [OS]). ORR included stringent complete response (sCR), complete response (CR), very good partial response (VGPR), and partial response (PR) per IMWG 2016 criteria. Minimal residual disease (MRD) negativity was assessed by multiparameter flow cytometry at a sensitivity of at least 10^{-5}.
Additionally, secondary endpoints included pharmacokinetics (CAR-T cell expansion kinetics quantified by qPCR and flow cytometry), pharmacodynamics (cytokine profiling and immune cell subsets). Pharmacokinetic parameters included maximum concentration (Cmax), time to peak (Tmax), and area under the curve from day 0 to day 28 ($AUC_{0-28}d$) of BCMA CAR-T cell expansion in peripheral blood following ESO-T01 infusion. qPCR was used to measure the copy number of lentiviral transgenes, with a validated detection limit of 50 copies per microgram of genomic DNA (Junke Zhengyuan). Pharmacodynamic evaluations included serial measurement of cytokines (IL-6, IL-10, IFN-γ, TNF-α and others), C-reactive protein, ferritin, immunoglobulin levels (IgG?IgA?IgM), and lymphocyte subsets (T, B, and NK cell frequencies and absolute counts) in peripheral blood.
Exploratory analyses included vector shedding, immunogenicity, off-target detection, and CAR-T cell insertion site analysis; based on the treatment response of the first patient, the conditioning protocol was adjusted and post-hoc analyses were conducted.

Plants

Seed stocks: not applicable

Novel plant genotypes: not applicable

Authentication: not applicable

Flow Cytometry

Plots

Confirm that:

☒ The axis labels state the marker and fluorochrome used (e.g. CD4-FITC).

☒ The axis scales are clearly visible. Include numbers along axes only for bottom left plot of group (a 'group' is an analysis of identical markers).

☒ All plots are contour plots with outliers or pseudocolor plots.

☒ A numerical value for number of cells or percentage (with statistics) is provided.

Methodology

Sample preparation: Peripheral blood samples from patients were analyzed using flow cytometry to assess the characteristics of CAR-T cells and their subsets.

Instrument: Flow cytometry samples were acquired using the BECKMAN flow cytometer (DxFLEX) for data collection and analysis.

Software: Data were analyzed with CytExpert, FlowJo and NovoExpress.

Cell population abundance: Typically stained 0.5 - 1×10^6 total PBMCs at each timepoint.

Gating strategy: The gating strategy is provided in the supplementary information.

☒ Tick this box to confirm that a figure exemplifying the gating strategy is provided in the Supplementary Information.

Magnetic resonance imaging

Experimental design

Design type: not applicable

Design specifications: not applicable

Behavioral performance measures: not applicable

Acquisition

Imaging type(s): not applicable

Field strength: not applicable

Sequence & imaging parameters: not applicable

Area of acquisition: not applicable

Diffusion MRI ☐ Used ☒ Not used

Preprocessing

Preprocessing software: not applicable

Normalization: not applicable

Normalization template: not applicable

Noise and artifact removal: not applicable

Volume censoring: not applicable

Statistical modeling & inference

Model type and settings: not applicable

Effect(s) tested: not applicable

Specify type of analysis: ☐ Whole brain ☐ ROI-based ☐ Both

Statistic type for inference: not applicable

(See Eklund et al. 2016)

Correction: not applicable

Models & analysis

n/a	Involved in the study
☒	☐ Functional and/or effective connectivity
☒	☐ Graph analysis
☒	☐ Multivariate modeling or predictive analysis